Rare earth mobility as a result of multiple phases of fluid activity in fenite around the Chilwa Island Carbonatite, Malawi

Emma Dowman[1,2,3] Frances Wall[2,3] Peter J. Treloar[1] and Andrew H Rankin[1]

[1] Department of Geography and Geology, Kingston University, Kingston-upon-Thames, KT1 2EE, UK
[2] Camborne School of Mines, University of Exeter, Penryn Campus, Penryn, TR10 9FE, UK
[3] The Natural History Museum, Cromwell Road, London, SW7 5BD, UK
Emma Dowman   emma@abdm.co.uk

Keywords:

fenite, rare earths, fluid inclusions, apatite

Abstract

Carbonatites are enriched in critical raw materials such as the rare earth elements (REE), niobium, fluorspar and phosphate. A better understanding of their fluid regimes will improve our knowledge of how to target and exploit economic deposits. This study shows that multiple fluid phases penetrated the surrounding fenite aureole during carbonatite emplacement at Chilwa Island, Malawi. The first alkaline fluids formed the main fenite assemblage and later microscopic vein networks contain the minerals of potential economic interest such as pyrochlore in high-grade fenite and RE minerals throughout the aureole. Seventeen samples of fenite rock from the metasomatic aureole around the Chilwa Island carbonatite complex were chosen for study (Natural History Museum, London collection BM1968 P37). In addition to the main fenite assemblage of feldspar and aegirine ± arfvedsonite, riebeckite and richterite, the fenite contains micro-mineral assemblages including apatite, ilmenite, rutile, magnetite, zircon, RE minerals and pyrochlore in vein networks. Petrography using SEM-EDX showed that the RE minerals (monazite, bastnäsite and parisite) formed later than the fenite feldspar, aegirine and apatite and provide evidence of REE mobility into all grades of fenite. Fenite apatite has a distinct negative Eu anomaly (determined by LA-ICP-MS) that is rare in carbonatite-associated rocks and interpreted as related to pre-crystallisation of plagioclase and co-crystallisation with K-feldspar in the fenite. The fenite minerals have consistently higher mid REE/light REE ratios (La/Sm = ~1.3 monazite, ~1.9 bastnäsite, ~1.2 parisite) than their counterparts in the carbonatites (La/Sm = ~2.5 monazite, ~4.2 bastnäsite, ~3.4 parisite). Quartz in the low- and medium-grade fenite hosts fluid inclusions, typically a few µm in diameter, secondary and extremely heterogeneous. Single phase, 2- and 3-phase, single solid and multi solid-bearing examples are present, with 2-phase the most abundant. Calcite, nahcolite, burbankite and barite were found in the inclusions. Decrepitation of inclusions occurred at around 200˚C

36 before homogenisation but melting temperature data indicate that the inclusions contain
37 relatively pure CO_2. A minimum salinity of around 24 wt.% NaCl equivalent was determined.
38 Among the trace elements in whole rock analyses, enrichment in Ba, Mo, Nb, Pb, Sr, Th
39 and Y and depletion in Co, Hf and V are common to carbonatite and fenite but enrichment
40 in carbonatitic type elements (Ba, Nb, Sr, Th, Y, and REE) generally increases towards the
41 inner parts of the aureole. A schematic model contains multiple fluid events, related to first
42 and second boiling of the magma, accompanying intrusion of the carbonatites at Chilwa
43 Island, each contributing to the mineralogy and chemistry of the fenite. The presence of
44 distinct RE mineral micro-assemblages in fenite at some distance from carbonatite could
45 be developed as an exploration indicator of REE enrichment.

46 ## Introduction

47 Carbonatites are the most important economic source of rare earth elements (REE). Most
48 carbonatites are characteristically enriched in REE compared to other rock types (Verplanck
49 and Van Gosen, 2011 and references therein), and some, such as Mount Weld, Australia;
50 Mountain Pass, USA; Bear Lodge, USA; Ngualla, Tanzania; Saint-Honoré, Canada;
51 Songwe Hill, Malawi and Lofdal, Namibia have high enough concentrations to constitute
52 ore deposits. The world's largest REE mine at Bayan Obo, China is also thought to be a
53 highly altered carbonatite (Smith, 2007). Rare earth ore deposits in carbonatites are
54 reviewed in Mariano, (1989); Lipin and McKay, (1989); and Chakhmouradian and Wall,
55 (2012). The economics of REE ore deposits depend very much on which of the REE are in
56 highest concentrations since the price of the REE varies greatly. Generally light REE (La-
57 Nd) are less valuable than mid (Sm- Gd) and heavy REE (Tb- Lu).
58
59 A better understanding of the fluid regimes and transport of light, mid and heavy REE in
60 and around carbonatite complexes is important in order to improve ore deposit models,
61 predict where to explore for the more expensive REE, and help to identify more
62 economically viable deposits.
63
64 Fenite is a typical rock around carbonatite and alkaline rock complexes. It forms in aureoles
65 of alkaline metasomatic alteration of the country rock around the carbonatite and alkaline
66 silicate intrusions. During the process of fenitisation, feldspar and alkali pyroxene and/or
67 amphibole usually are produced, at the expense of quartz and original feldspar components.
68
69 Fenitisation is usually progressive with gradational boundaries between fenite and
70 unaltered country rock and, generally, an increasing intensity of alteration towards the
71 intrusion. Fenite aureoles frequently comprise an outer sodic zone and an inner potassic

fenite (Le Bas, 2008). Sodic fenitisation is generally considered to precede potassic fenitisation, although the causes of this relatively common pattern have not been fully determined. Both calcitic and ankeritic carbonatites can induce both Na- and K-rich fluids (Le Bas, 2008), which suggests that the composition of the parent magma is not the main determining factor, although the magmatic evolution of any individual carbonatite may control the earlier preferential loss of Na over K (Woolley, 1982). A dependence of type of alkaline alteration on magma temperature appears to be important, with sodic fenite being associated with magma at deeper levels in the complex, of higher temperature, and possibly with a lower CO_2 content. In contrast, potassic fenite may be produced from magma at higher levels and lower temperatures, and be richer in CO_2 (Le Bas, 2008; Woolley, 1982; Rubie and Gunter, 1983; Viladkar, 2012). Previous studies of the fenitisation process include Morogan and Woolley, (1988); Morogan, (1989); Verschure and Maijer, (2005); Platt and Woolley, (1990); Woolley, (1969); Garson and Campbell Smith, (1958); Carmody, (2012); Andersen, (1989); McKie, (1966). An improved knowledge of fenitisation processes is key to understanding the exsolution and evolution of the fluids exsolved from the alkaline content of carbonatite magmas.

It is well accepted that REE move from carbonatite magma into the fenite aureole. Martin et al., (1978) made one of the first studies of REE mobility into fenite when they identified mobilisation of rare earths into a barren quartzite rock by magma-derived during the emplacement of the Borralan alkaline/carbonatite complex in Scotland. Bühn and Rankin, (1999) investigated element partitioning at the Kalkfeld carbonatite in Namibia. They remarked on the high capability of H_2O-CO_2-Cl-F fluids to transport the LILE and HFSE at high temperatures, and developed a qualitative retention series of elements in the fluid as follows: Cl=Na>K>(Cs,Rb,Pb,Cu,Zr)>U=Th>Ti>Y=Ba>F=Mg>REE=Sr>Mn=Fe which represents an increasing tendency from right to left to partition into the fluid relative to the crystallising carbonatite melt. The incompatible behaviour of the REE has become generally accepted, although it is acknowledged that the partitioning in natural magma systems is highly complex and only reasonably well understood for a few geochemically simple systems (Chakhmouradian and Reguir, 2013).

Until recently, apatite was the only mineral mentioned in literature on rare-earth-bearing minerals in fenite around carbonatites (Le Bas, 2008; Smith, 2007; Andersen, 1989; Morogan, 1989; Morogan and Woolley, 1988; Kresten and Morogan, 1986). However, increasing interest in REE mineralisation in altered rocks, such as fenites, has led to recent reports of rare-earth (RE) minerals. Cordylite-(La), a new mineral species was found in fenite from the Biraya Fe-REE deposit in Irkutsk, Russia (Mills et al., 2012), associated with

109 many other RE-minerals, such as daqingshanite-(Ce),(La), monazite-(Ce) and bastnäsite-
110 (Ce). Fenite at the Songwe carbonatite complex in Malawi has also been identified as
111 HREE-enriched, including occasional xenotime-(Y) (Broom-Fendley et al., 2013). At
112 Bandito in the Yukon, a fenite (associated with nepheline syenite rather than carbonatite) is
113 also RE-rich, with up to 3.49% TREO+Y in highly metasomatised syenite, which contains
114 minerals such as monazite, bastnäsite and apatite (Endurance Gold Corporation, 2012,
115 2013).
116
117 Previous studies of fluid inclusions related to fenites have demonstrated that fenitising fluids
118 are generally aqueous-CO_2-bearing, alkali-bicarbonate brines of variable salinity, capable
119 of carrying the REE, large-ion-lithophile elements and HFSE (Palmer, 1998; Bühn and
120 Rankin, 1999; Bühn et al., 1999, 2001; Williams-Jones and Palmer, 2002; Carmody, 2012).
121
122 Chilwa Island contains the whole range of calcite, dolomite and Fe-rich carbonatites
123 (Garson and Campbell Smith, 1958), together with a well-formed fenite aureole containing
124 sodic and potassic fenite. Hence, it is often featured in textbooks. RE minerals are present
125 in the carbonatite, although the complex has not been considered as an important REE
126 source. This study provides new evidence of REE mobility into fenite being a second stage
127 process of mineralisation rather than accompanying the first alkali metasomatism. We
128 present evidence of micromineral assemblages within the main mineral assemblage of the
129 fenite at Chilwa Island. Variable RE signatures of whole rock analyses of fenite and
130 carbonatite and an investigation of the fluid inclusions in fenitic quartz are combined to
131 propose a new model for the metasomatic regime around the carbonatite.

132 ## Approach and methodology
133 Our new data, which permit a full interpretation of the Chilwa Island Complex, are presented
134 below. Samples used are from the Natural History Museum, London collection BM1968 P37.
135 Analyses used SEM-EDS, SEM-based CL, LA-ICP-MS and fluid inclusion-based
136 techniques. Full details of analytical techniques are available as supplementary data.
137

Geological background

The carbonatite complex of Chilwa Island lies in the Cretaceous-aged Chilwa Alkaline Province at the extreme southern end of the East African Rift system The area has seen repeated emplacement of alkaline and carbonate rocks into amphibolite and granulite facies basement rocks (Bailey, 1977; Kröner et al., 2001). Crustal extension and decompressional melting between 138 and 107 Ma drove alkaline magmatism in the CAP (Eby et al., 1995), producing seventeen carbonatite intrusions, in two main belts: a western belt associated with lines of rifting and an eastern chain within a zone of depression (Garson, 1965).

Chilwa Island is located at the north of the eastern chain of carbonatites, in the southwest of Lake Chilwa. The largest of the Malawi carbonatites, it is a ring complex ca. 4 km in diameter, consisting of multiple carbonatite intrusions. Structural relationships indicate sequential emplacement from early outer calciocarbonatites (commonly termed 'sövite') inwards to later ankeritic (increasing Mg, Fe) carbonatites and then the youngest central sideritic (Fe, Mn-rich) carbonatite (Garson and Campbell Smith, 1958; Garson, 1965; Le Bas, 1981; Woolley, 2001). Brecciated country rock and fenitised Precambrian granulites surround the carbonatite rocks (Figure 1). The outer margins of alteration of the country rock are hidden beneath the lake and its sediments. No unaltered rock is found on the island, and therefore little is known of the original rocks. A time frame for the complex is provided by K-Ar dating of biotite in the earliest (calcio)carbonatite by Snelling, (1965) at 138 Ma. Eby et al., (1995) used titanite fission-track analysis to date a nepheline-syenite plug intruding carbonatite at 126 Ma, with apatite fission-track dates of 87±9 Ma from the same rock. This accords with fission-track dating of carbonatite-derived apatite in fenite (Dowman, 2014), which yielded an age of 99±4 Ma.

163

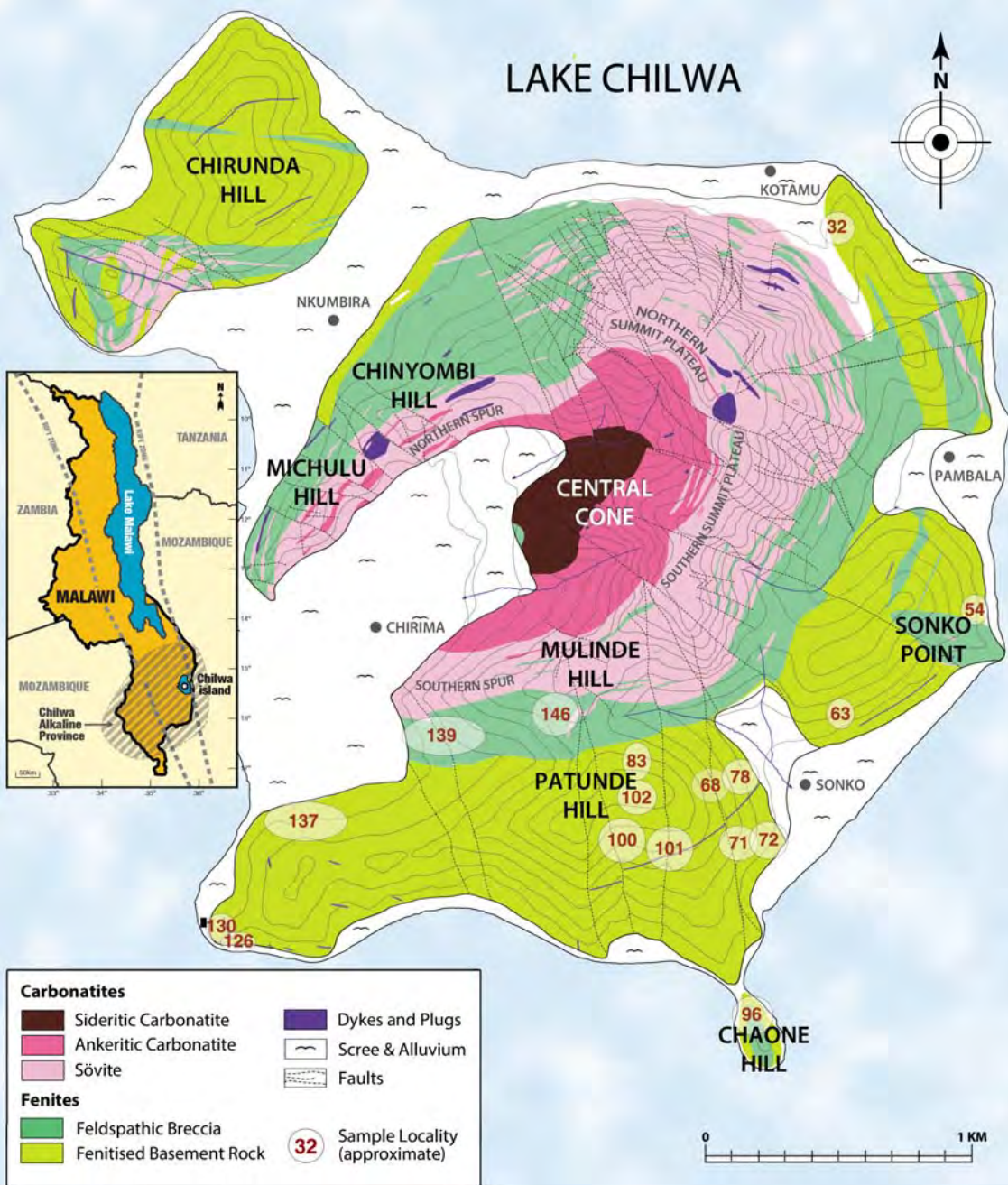164   **Fig. 1**   Geological map of Chilwa Island carbonatite complex [adapted from Garson and Campbell Smith
165   (1958)].
166   Numbers are approximate locations of fenite samples used in study

167

LAKE CHILWA

N

CHIRUNDA HILL

KOTAMU

32

NKUMBIRA

NORTHERN SUMMIT PLATEAU

CHINYOMBI HILL

NORTHERN SPUR

MICHULU HILL

PAMBALA

CENTRAL CONE

SOUTHERN SUMMIT PLATEAU

SONKO POINT

54

CHIRIMA

MULINDE HILL

63

SOUTHERN SPUR

146

139

PATUNDE HILL

83
102

68 78

SONKO

137

100 101

71 72

130
126

CHAONE HILL

96

Inset map:

N

TANZANIA

RIFT ZONE

ZAMBIA

MOZAMBIQUE

Lake Malawi

MALAWI

MOZAMBIQUE

Chilwa island

Chilwa Alkaline Province

50km

Legend:

Carbonatites

- Sideritic Carbonatite
- Ankeritic Carbonatite
- Sövite
- Dykes and Plugs
- Scree & Alluvium
- Faults

Fenites

- Feldspathic Breccia
- Fenitised Basement Rock
- (32) Sample Locality (approximate)

0   1 KM

Mineralogy of the Chilwa Island Carbonatite Complex

Garson and Campbell Smith, (1958) undertook a comprehensive survey of the mineralogy of the complex. They described sövite carbonatites as varying from almost purely calcite to compositions containing apatite or pyroxene. Minerals found in both sövite and ankeritic carbonatite include pyrochlore, magnetite, feldspar, quartz and barite. Synchysite and florencite are RE-bearing minerals occurring occasionally in these carbonatites. The central sideritic carbonatite is described as being of secondary origin (Woolley, 2001), and is a rock rich in Fe- and Mn-oxides, characterised by numerous druses and veinlets that are lined with minerals such as quartz, calcite and barite. The RE-bearing minerals, florencite and bastnäsite were identified within some of these druses.

The outermost carbonatite, sövite, is surrounded by a collar of potassic feldspathic breccia. The breccias are the end-stage or high-grade fenite, probably broken up during episodes of high pressure in the history of the carbonatite central complex. Outside the breccia lies fenitised country rock, divided by Woolley, (1969) into a less fenitised group of 'quartz fenites' and an inner group of 'syenitic fenites'. The mineralogy of the less altered quartz fenites is inherited primarily from the basement and is dominated by plagioclase and quartz, with minor aegirine also present. In the syenitic fenites, quartz and plagioclase are being replaced by a new mineralogy of orthoclase, aegirine and sodic amphiboles, with magnesioarfvedsonite being identified in syenite fenite, and riebeckite in quartz fenite. No RE-minerals are described in any type of fenite.

Garson and Campbell Smith, (1958) proposed metasomatism of the aureole by several waves of fenitisation. This alteration was through fluids channelled along a network of veins and grain boundaries throughout the rocks. Woolley, (1969) made a distinction between the potassic breccias and the more sodic outer aureole, attributing the cause to fluids that were temporally separated, and probably from different sources. Both Garson and Campbell Smith, (1958) and Woolley, (1969) interpret fenite mineralogy, including the presence of apatite in veins of alteration, as being an indicator that fenitising solutions were probably rich in water and CO_2, and that they carried K, Fe and Na cations, and mobilised P_2O_5.

In addition to the evident metasomatism of the outer parts of the complex, the sideritic carbonatite rocks may also have undergone secondary alteration (Garson and Campbell Smith, 1958) as a result of oxidation, and areas of sövite may have been replaced by more ankeritic carbonatite. A late-stage hydrothermal and silicification event, associated with the final waning of carbonatite activity, probably affected all parts of the complex in a selective manner, with some rocks being replaced, and others remaining unchanged. Si was

205 probably mobilised from the country rocks, and alteration introduced secondary minerals,

206 such as quartz, calcite and barite, as described in druses in the core sideritic carbonatite,

207 as well as quartz and quartz-fluorite veins in both carbonatite and fenite rocks.

208

Mineralogy of the fenite aureole

210 For this paper, a straightforward scheme to distinguish the fenite rocks is required. Although

211 not ideal, because alteration can often form a continuum, the terminology of low-grade and

212 medium-grade fenite as used here reflects relative intensity of metasomatism, and

213 approximately matches the earlier petrographic descriptions of Garson and Campbell Smith,

214 (1958) and Woolley, (1969) of 'quartz fenite' and 'syenite fenite'. Low-grade fenite at Chilwa

215 Island generally comprises less than 10% veins of aegirine/iron oxide alteration, and high-

216 grade fenite refers to rocks with a monophase matrix of either orthoclase or secondary

217 quartz.

218

219 Low-grade fenite has a matrix of quartz and plagioclase. Feldspar exhibits both perthitic

220 and antiperthitic textures. Samples from this fenite grade provide a few examples of

221 magnetite containing a trelliswork of ilmenite (Figure 2a) but veins are scarce, and where

222 present, are usually of aegirine and K-feldspar. Some apatite, rutile and ilmenite

223 assemblages are present in which minerals show porosity, but rarely any zoning. Monazite,

224 although not common, is the only RE-mineral that occurs regularly, usually in association

225 with apatite. Parisite, xenotime and pyrochlore appear to be very rare in this part of the

226 aureole, only being found in one sample.

227

228 The medium-grade fenite group contains several samples that appear more strongly altered,

229 and they are treated here as a subgroup of medium/high-grade rocks. The matrix of the

230 majority of medium-grade fenites is still feldspar and quartz, but the feldspar is increasingly

231 turbid, rarely exhibiting perthitic textures, and quartz is a less important phase than in the

232 low-grade fenite. Some evidence of secondary quartz is indicated adjacent to areas of

233 aegirine alteration. Aegirine mineralisation is more extensive, being concentrated in veins

234 often fringed by K-feldspar, which is now a more common mineral. The main characteristic

235 of this grade of fenite is seen within these veins, especially the presence of micro-

236 assemblages of ilmenite, fluorapatite and zircon, which were found in every medium-grade

237 sample (Figure 2b). Ilmenite grains frequently show areas of Fe-rich and Ti-rich separation,

238 and are often associated with magnetite grains and occasionally with Nb-bearing rutile

239 grains (Figures 2c and 2d). Apatite is now rarely porous, and displays strong zoning.

240 Amphibole (magnesioarfvedsonite, richterite) was detected in some sections, invariably

241 associated with aegirine. Rare earth minerals occur regularly in the areas of mineralisation.

242 Monazite is the most common of these, often in the form of rim grains in apatite. Bastnäsite,
243 typically shard-like in form, is also present, but is rarer than monazite. Parisite and xenotime
244 are scarce and only noted in a few sections, as was carbonate, which usually has a
245 composition of calcium, or more rarely, ankeritic carbonate.

246

247 The more altered subgroup within the medium-grade fenites is dominated by a mineralogy
248 of aegirine and K-feldspar (orthoclase), with an increasing presence of recrystallised quartz.
249 Only vestiges of the ilmenite-apatite-zircon microassemblages remain. Apatite is now much
250 scarcer, and exhibits no zoning or any association with monazite. Sodic amphiboles
251 (magnesioarfvedsonite, richterite) are found together with aegirine, but in no greater
252 abundance than in the less fenitised members of this group. Zircon, usually located in
253 aegirine, appears ragged in shape with signs of resorption (Figure 2e). A greater variety of
254 trace phases is seen, such as barite, pyrite, carbonates (a few examples of both calcium
255 carbonate and ankeritic carbonate) and also the Ca-bearing RE fluorcarbonate parisite-(Ce)
256 (Figure 4a), although the RE minerals monazite and bastnäsite are absent.

257

258 The pink colour of the breccia (high-grade fenite) reflects its almost monophasic K-feldspar
259 composition. The microassemblages and aegirine of the medium-grade fenite are absent,
260 although secondary quartz is still found. Pyrochlore is now present, usually associated with
261 increasingly ragged zircon grains (Figure 2f), and goyazite was detected in thread-like veins.
262 An unidentified Th-rich RE mineral was found, but no carbonate was present.

263

264 The highest-grade fenite is represented by sample BM1968 P37 83. This is also an almost
265 monophasic rock, but, in contrast to the breccia, is composed of secondary quartz. No
266 feldspar of any variety was seen in this section. Other minerals in the section are
267 assemblages of apatite and pyrochlore, the latter often rich in Pb. The apatite is often
268 associated with RE minerals, such as monazite-(Ce),(La), xenotime and an unidentified Th-
269 MREE phase (Figure 4b). Bastnäsite-(Ce) and zoned goyazite were seen in areas of
270 pyrochlore mineralisation.

271
272   **Fig. 2** Back-scattered electron images of fenites from Chilwa Island
273   a)   magnetite with ilmenite in low-grade fenite BM1968 P37 130
274   b)   typical mineral assemblage of apatite, zircon and ilmenite in medium-grade fenite BM1968 P37 78
275   c)   Ilmenite showing rutile-magnetite separation in medium-grade fenite BM1968 P37 96
276   d)   Ilmenite associated with magnetite, also apatite and zircon in medium-grade fenite BM1968 P37 101
277   e)   Zircon resorbing in aegirine in medium/high-grade fenite BM1968 P37 54
278   f)   Pyrochlore and zircon association in breccia BM1968 P37 146
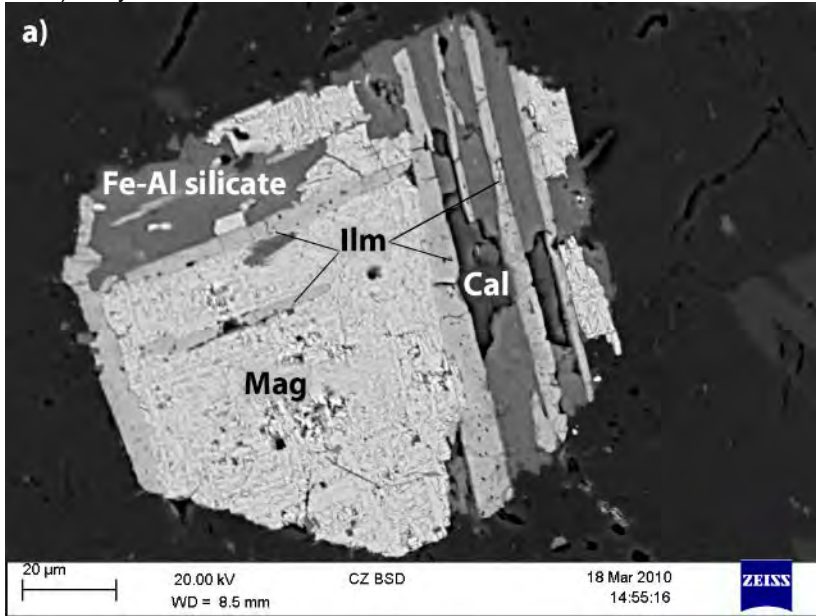
279
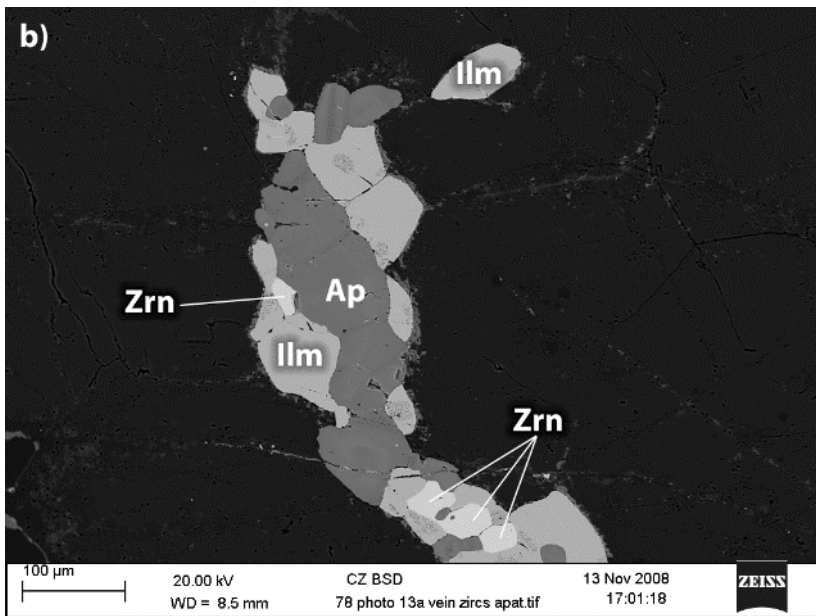
280
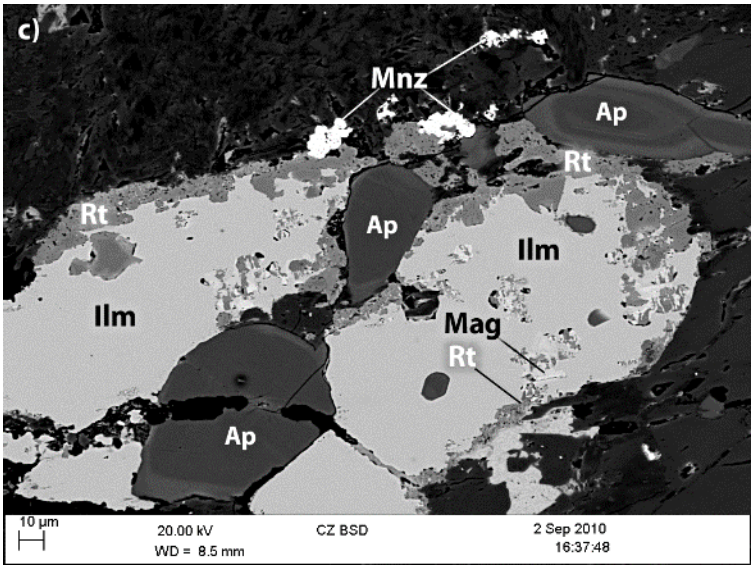
281
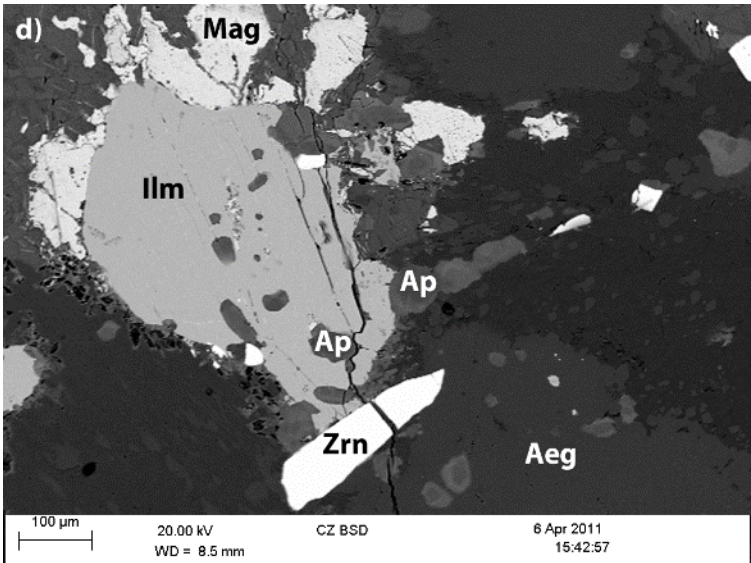
282
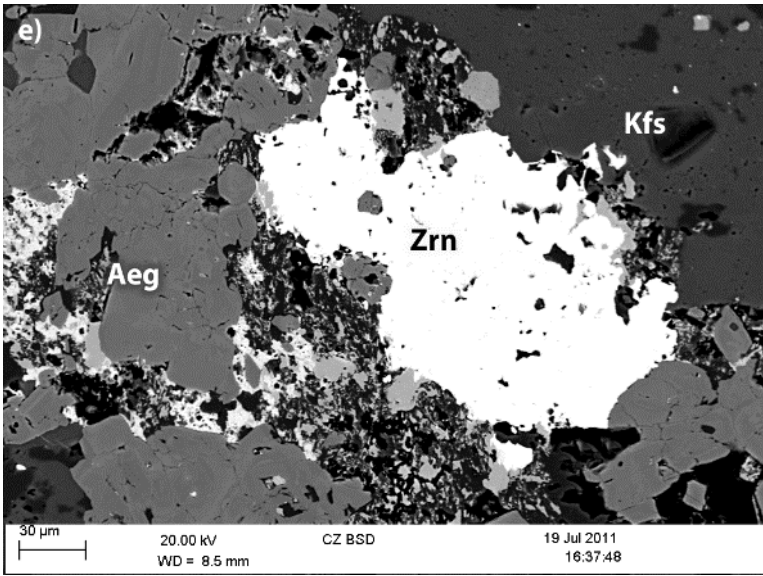
283
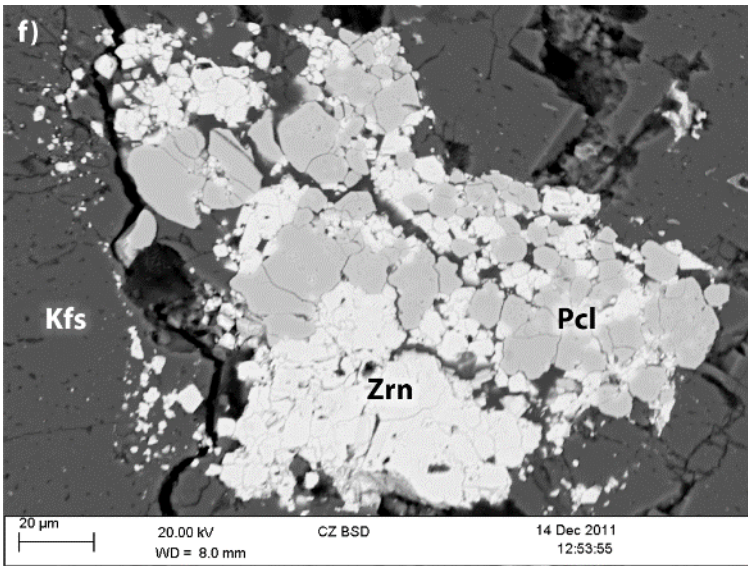
284

285 The mineralogical data are summarised in Table 1 and Figure 3a. Figure 3a illustrates in a
286 qualitative way the relative abundance of different minerals across the fenite aureole.
287 Figures 3b and 3c (from whole-rock analyses) indicate the quantitative variation of major
288 elements (by wt. %) and selected trace elements (chondrite-normalised) in the composition
289 of each fenite zone.

290

291 **Table 1** Summary of mineralogy in fenite zones at Chilwa Island

Fenite grade	Matrix	Fenite mineral assemblages	Apatite habit	Carbonates, sulfides	RE minerals
Low-grade	Plagioclase with minor orthoclase. Perthite common. Quartz 25-30%.	A few veins of aegirine (<10%), occasionally accompanied by apatite, zircon, ilmenite , rutile and amphibole. Magnetite grains, some with 'ilmenite trellis'.	Absent, or a few grains per section. Some porous, but zoning rare. Occasionally contain monazite inclusions.	Rare carbonate veins, variable Ca, Fe, Mn content. Small grains of barite common to absent. One section contained a few grains of pyrite and a single galena.	Monazite-(Ce) with Th found in each section. Rare parisite-(Ce), and one xenotime grain in one section.
Medium-grade	Plagioclase is dominant, orthoclase forming around mineralised areas. Perthite rarely seen. Quartz typically 20-25%.	Veins of aegirine form 15-20% of section, associated with microassemblages of ilmenite/apatite/zircon, often also Nb-bearing rutile. Ilmenite separation into Fe and Ti phases. Magnetite grains in most sections, sometimes with 'ilmenite trellis'. Na-amphibole found amongst aegirine grains.	Common part of micro-assemblages. Typically zoned and with RE minerals (mostly monazite) inclusions. Rare submicron zircon inclusions.	Most sections contain common small barite grains and occasional pyrite. Carbonate rare, may be of calcite or ankerite.	Monazite-(Ce) is most common, more abundant than in low-grade fenite. Bastnäsite-(Ce) also occurs. One example of xenotime-(Y) seen, also one unidentified REE-Th-Sr carbonate phase.
Medium/high grade	Feldspar dominated by orthoclase. No perthite. Primary quartz rare.	Aegirine mineralisation typically 45-60%. Amphibole and Nb-rutile are present but microassemblages of ilmenite/apatite/zircon are rare or absent. Secondary quartz forms up to 10% of section. A few pyrochlore grains now present.	Less frequent as fenite grade increases. When present, rarely zoned, and without RE mineral inclusions.	Frequent small barite grains. A few pyrite grains. Carbonate (mostly calcite, but also ankerite) may occur with recrystallised quartz.	Monazite and bastnäsite rare or absent. Parisite-(Ce) present in most sections.
Breccia	Orthoclase	No aegirine. Small areas of recrystallised quartz. Occasional assemblages of zircon and pyrochlore. Pyrochlore may be Pb, U-bearing.	Absent.	None found.	Unidentified REE-Th phosphate phase, also goyazite.
BM1968 P37 83	Recrystallised/ secondary quartz. Feldspar absent.	Assemblages of apatite and (plumbo)pyrochlore. A small number of Nb-rutile and magnetite grains. No zircon.	Sometimes with porous outer zone containing RE minerals.	Small grains of barite, some Mn-bearing.	Monazite-(Ce), (La), bastnäsite-(Ce), xenotime-(Y) and unidentified REE-Th-rich phosphate phase.

292

293

294 **Fig. 3**
295 a) Qualitative distribution of minerals in fenite zones at Chilwa Island
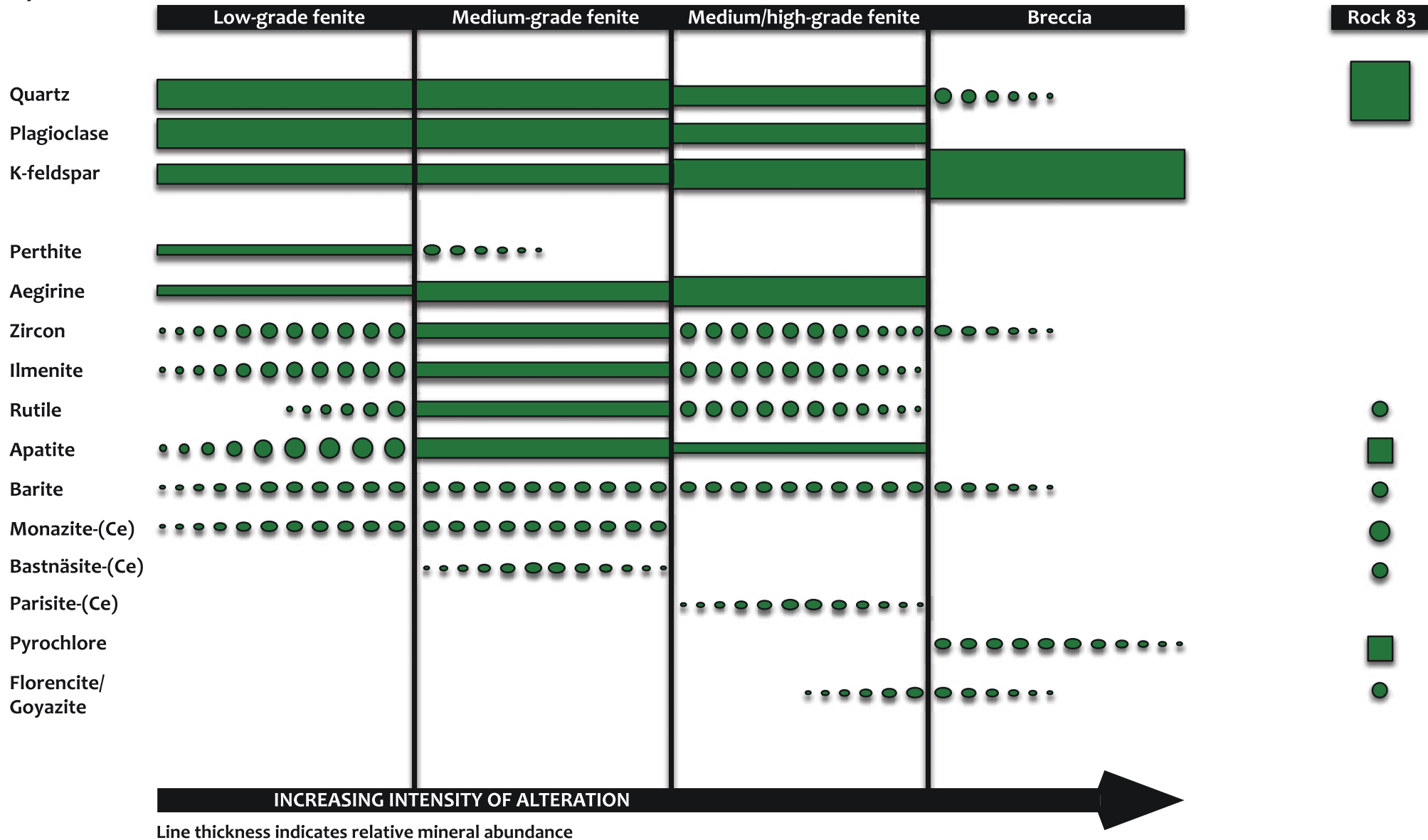296 b) Distribution of major elements by wt. % in fenite zones at Chilwa Island
297 c) Concentration/chondrite abundance of selected trace elements in fenite zones at Chilwa Island
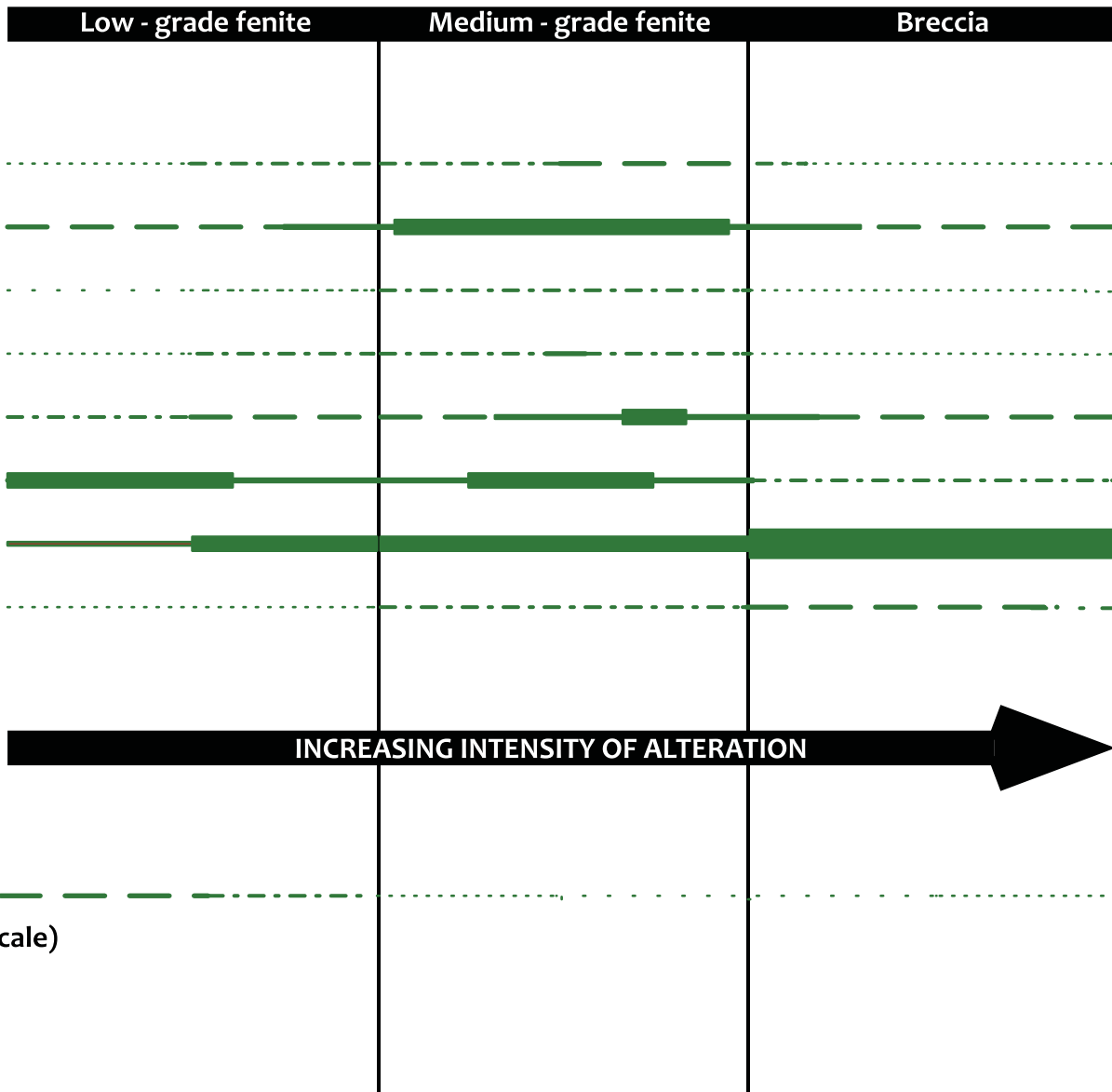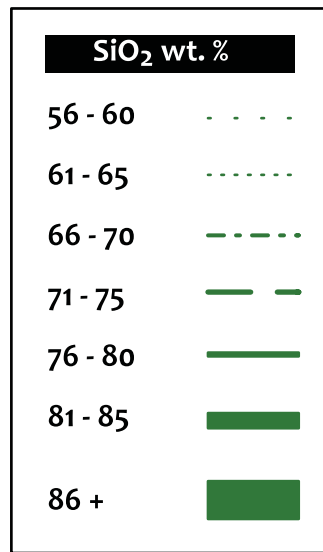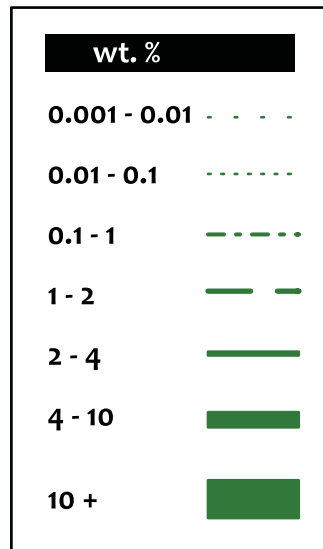298

a)

	Low-grade fenite	Medium-grade fenite	Medium/high-grade fenite	Breccia

Quartz
Plagioclase
K-feldspar

Perthite
Aegirine
Zircon
Ilmenite
Rutile
Apatite
Barite
Monazite-(Ce)
Bastnäsite-(Ce)
Parisite-(Ce)
Pyrochlore
Florencite/
Goyazite

INCREASING INTENSITY OF ALTERATION

Line thickness indicates relative mineral abundance

Rock 83

b)

Chilwa Island major elements wt. %

	Low - grade fenite	Medium - grade fenite	Breccia	BM1968 p37 83

TiO_2

Fe_2O_3 (t)

MnO

MgO

CaO

Na_2O

K_2O

P_2O_5

INCREASING INTENSITY OF ALTERATION

SiO_2

(note different scale)

wt. %	
0.001 - 0.01	
0.01 - 0.1	
0.1 - 1	
1 - 2	
2 - 4	
4 - 10	
10 +	

SiO_2 wt. %	
56 - 60	
61 - 65	
66 - 70	
71 - 75	
76 - 80	
81 - 85	
86 +	

c)

Chilwa Island trace elements

| Low - grade fenite | Medium - grade fenite | Breccia | BM1968 p37 83 |

Rb, Ba, Th, U, Pb, Sr, Zr, Hf, Nb, Y, Total REE

INCREASING INTENSITY OF ALTERATION

conc^n/chondrite

- 0.1 - 25
- 26 - 50
- 51 - 100
- 101 - 200
- 201 - 300
- 301 - 400
- 401 - 1000
- > 1000
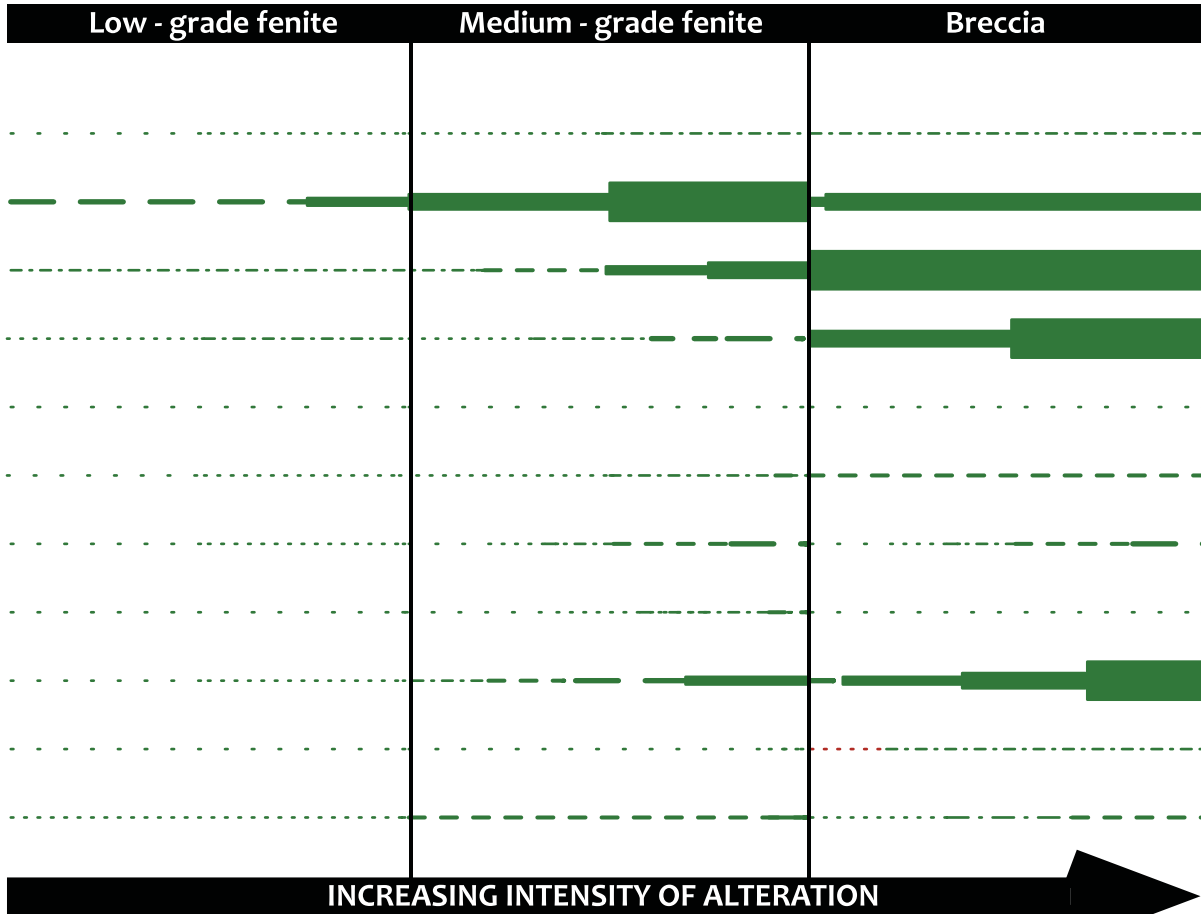
Carbonatite mineralogy

Four carbonatite samples have been studied and their mineralogy is summarised in Table 2. Ankerite with Mg>Fe and calcite are the dominant minerals together with one or more of apatite, pyrochlore and quartz. Parisite-(Ce), bastnäsite-(Ce), monazite-(Ce), and florencite-goyazite are all present as accessory phases (Figures 4c-4f).

Table 2 Summary of mineralogy of carbonatite sections from Chilwa Island

| Carbonatite	Matrix minerals	Accessory minerals
Ankeritic sövite 1957 1056 102	Calcium carbonate Apatite Ankeritic carbonate Ca>Mg>Fe>Mn	Parisite-(Ce), contains Th Goyazite-florencite Pyrochlore, contains Ce, Pb and Th Xenotime Nb-bearing rutile Barite
Pyrochlore-bearing ankeritic carbonatite 1957 1056 118	Ankeritic carbonate Ca>Mg>Fe>Mn Apatite Pyrochlore (with Ce, Y, Th)	Quartz Calcium carbonate Parisite-(Ce), contains Th Strontianite Barite
Ankeritic carbonatite 1957 1056 128	Ankeritic carbonate Ca>Fe>Mg>Mn Quartz K-feldspar	Strontianite Nb-bearing rutile Apatite Bastnäsite-(Ce) contains Th Monazite-(Ce), contains Th Parisite-(Ce), contains Th Goyazite-florencite Pyrite Barite
Sideritic carbonatite 1957 1056 113	Fe-Mn oxides Calcium carbonate Quartz	Th-RE carbonate Goyazite-florencite Synchysite-(Ce), contains Th

15

308
309
310
311 **Fig. 4** Back-scattered electron images of REE-bearing minerals at Chilwa Island
312   a) Vein of quartz and calcite containing parisite and barite in medium/high-grade fenite
313   BM1968 P37 54
314   b) Apatite with associated monazite, xenotime and unidentified Th-MREE phase in high-grade fenite
315   BM1968 P37 83
316   c) Strontianite with bastnäsite inclusions, and goyazite and rutile grains in ankeritic carbonatite
317   1957 1056 128
318   d) Parisite and pyrochlore in sövite and ankeritic carbonate 1957 1056 102
319   e) Mineralisation in 'sideritic' carbonatite 1957 1056 113
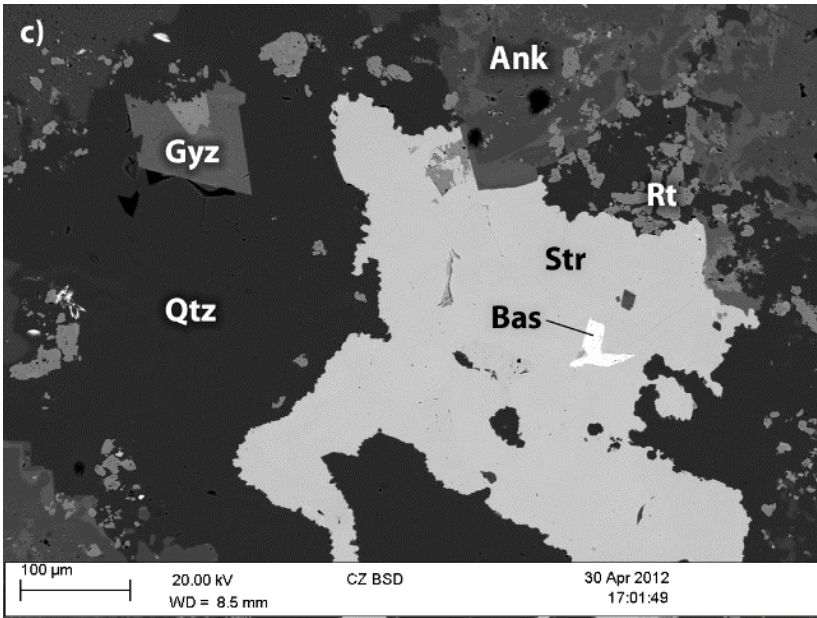320   f) Detail of unidentified Th-rich REE phase in 'sideritic' carbonatite 1957 1056 113
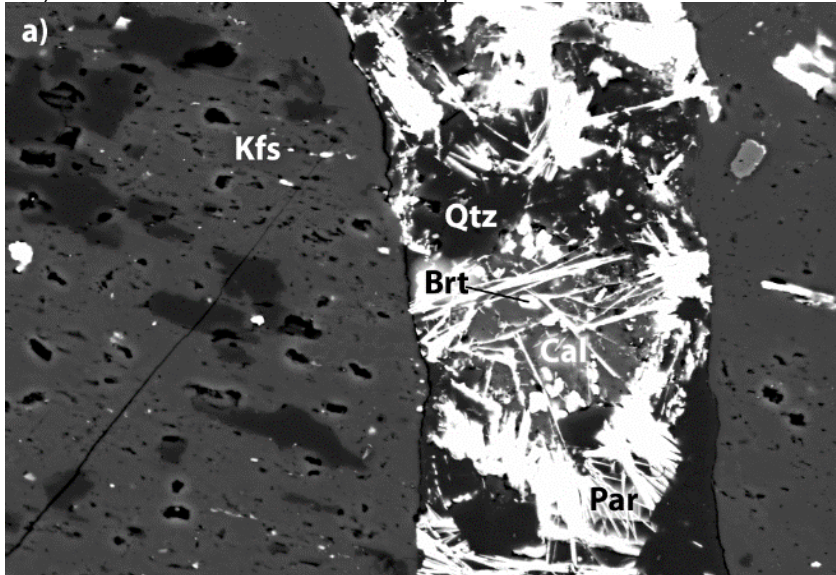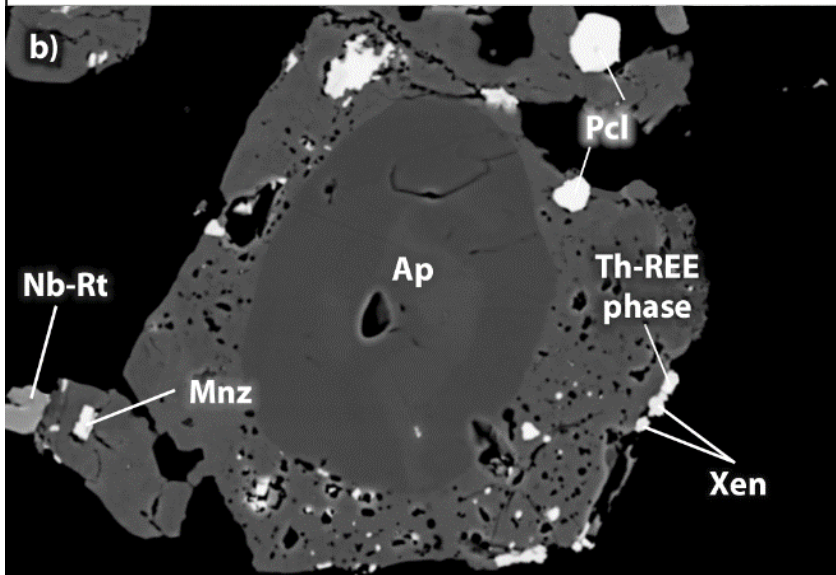
321

322
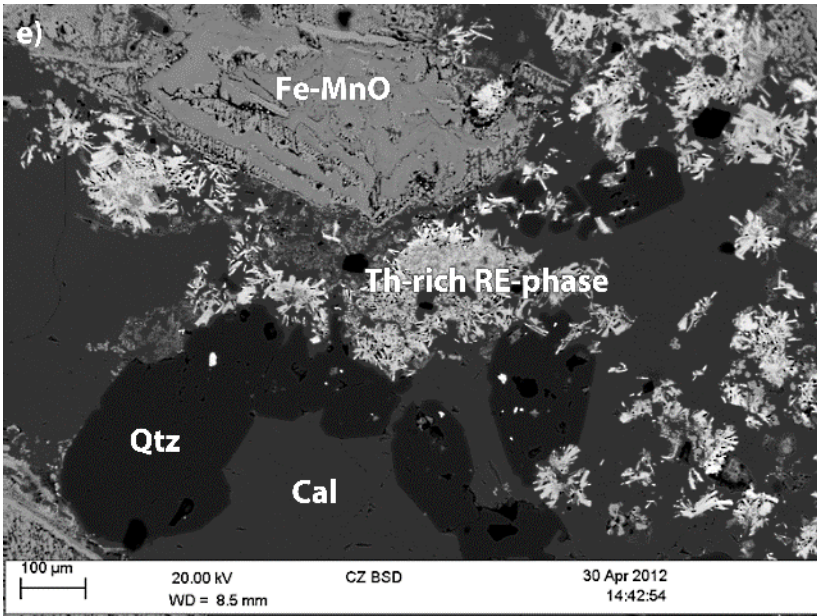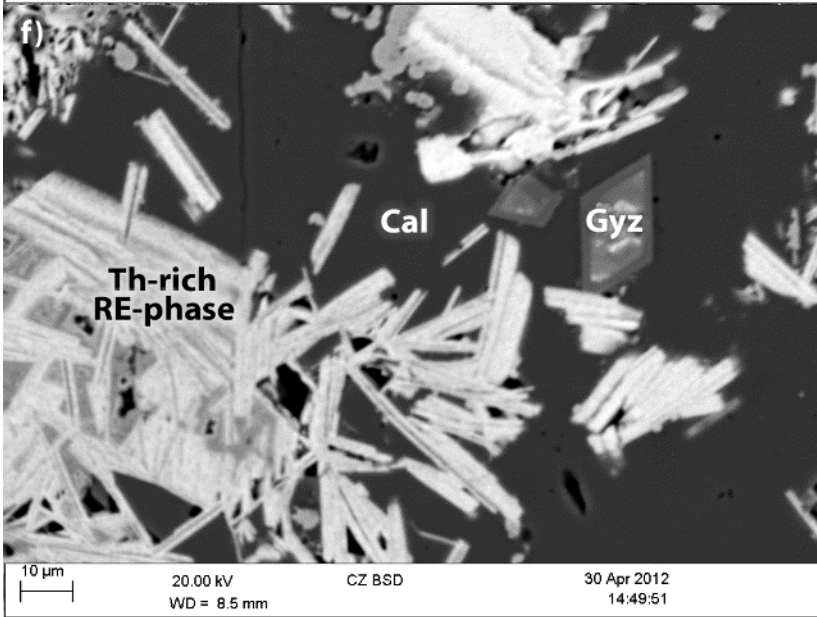
323

324

325

326
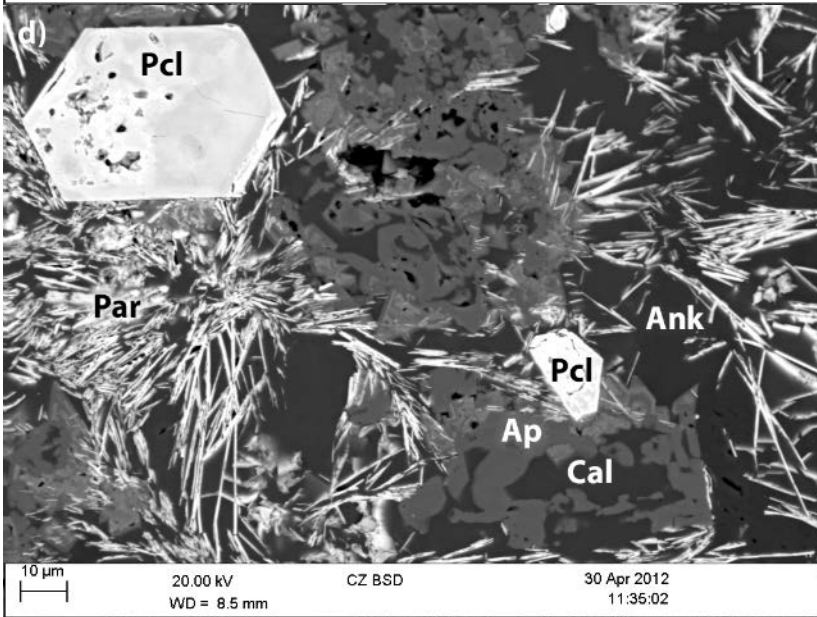
Apatite

Apatite is an important mineral at Chilwa Island where it is found in both fenites and carbonatites.

Apatite in fenite

In low-grade and medium-grade fenite, apatite is characteristically a vein-hosted mineral. Apatite-bearing veins are scarce in low-grade fenite, where apatite is typically unzoned and porous (Figure 5a), sometimes with monazite inclusions. Under cathodoluminescence, it luminesces in shades of purple, and is often associated with scarlet-luminescing K-feldspar (Dowman, 2014). The red luminescence of the feldspar is characteristic of fenitisation processes, and is attributed to the incorporation into the mineral of the activator, Fe^{3+}, which is contained in fenitising fluids of high alkalinity and of moderate to high temperature. In non-alkaline rocks, K-feldspar luminesces bright blue (Mariano et al., 1973; Mariano, 1978; 1988).

The porous appearance of apatite both in this low-grade fenite, and in the high-grade fenite BM1968 P37 83 (Figure 4b), may be the result of incipient dissolution or resorption of grains. Apatite is a much more common phase in medium-grade fenite, where it is typically found in fine-grained assemblages together with zircon, ilmenite, magnetite and rutile. Monazite inclusions and multiple concentric zones are characteristic of apatite in this zone (Figure 5b). Zones vary in number, thickness and sequence, but the most common BSE signature has a dark centre, surrounded by very bright zones, with a rim of intermediate brightness. CL images show the zones as different shades of purple and highlight the location of this mineral in areas of metasomatic alteration, as evidenced by the ubiquitous presence of K-feldspar (Dowman, 2014). Chemical mapping of a strongly zoned grain shows that the bright zones are REE-rich and relatively Ca- and P-impoverished (Figure 6).

Apatite persists into the medium/high-grade fenites, where the fine-grained assemblages of the medium-grade zone disappear. Here, apatite commonly occurs together with calcium carbonate, and continues to be a relatively common phase, but displays neither zoning nor porosity, and does not contain monazite inclusions (Figure 5c). However, apatite is absent where a higher intensity of metasomatism has produced rocks dominated by either aegirine and K-feldspar, such as in the most fenitised medium/high-grade fenite, BM1968 P37 137, or as in the high-grade breccia, by K-feldspar alone.

The unusual sample, BM1968 P37 83, is also strongly metasomatised, but alteration has created a mineralogy of drusy recrystallised quartz instead of K-feldspar. Apatite is present as a minor phase in this rock, and is found most commonly in association with pyrochlore

364   (Figure 5d). Grains typically display a porous, inclusion-rich outer zone and a clean inner

365   zone, but zoning caused by variation of REE content, typical of apatite in medium-grade

366   fenite, is absent.

367

368   Apatite is a common phase in all carbonatite sections apart from the sideritic sample (1957

369   1056 113), where it is completely absent. The ankeritic sövite 1957 1056 102 contains

370   apatite that is intricately intergrown with calcium carbonate and is associated with

371   pyrochlore and parisite (Figures 4d and 5e). In sample 1957 1056 118, apatite is abundant,

372   and also appears with pyrochlore, and ankeritic carbonate (Figure 5f).

373

374   Zoning in apatite in carbonatite is not common and was only seen in a small number of

375   separated grains from sövite 1957 1056 59, where concentric zoning was generally of a

376   less complex nature than that seen in apatite in medium-grade fenite. CL imaging reveals

377   a bluer hue than that seen in apatite in fenite, but the association of apatite with K-feldspar

378   was again apparent (Dowman, 2014). Carbonatitic apatite appears to lack a strong

379   association with monazite, and inclusions found in apatite grains from 1957 1056 59 were

380   of calcite. A few inclusions of barite and strontianite were seen in apatite of the pyrochlore-

381   rich carbonatite, 1957 1056 118.

382

383
384
385
386 **Fig. 5** Back-scattered electron images of apatite in fenite and carbonatite at Chilwa Island
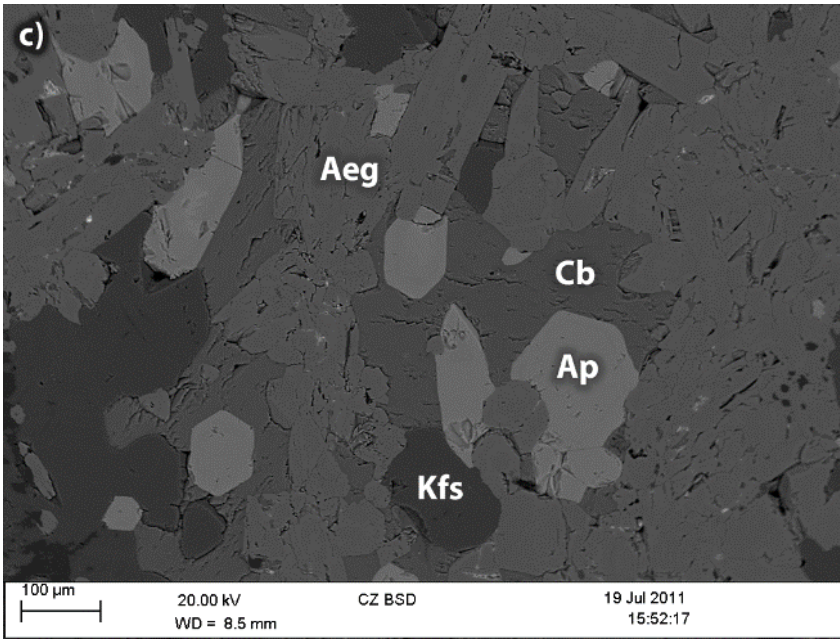387   a)   Porous, unzoned apatite in low-grade fenite BM1968 P37 72
388   b)   Zoned apatite in medium-grade fenite BM1968 P37 78
389   c)   Unzoned apatite in medium/high-grade fenite BM1968 P37 68
390   d)   Apatite associated with pyrochlore in high-grade quartz-rich rock BM1968 P37 83
391   e)   Apatite associated with calcite in ankeritic sövite 1957 1056 102
392   f)   Apatite associated with pyrochlore in ankeritic carbonatite 1957 1056 118
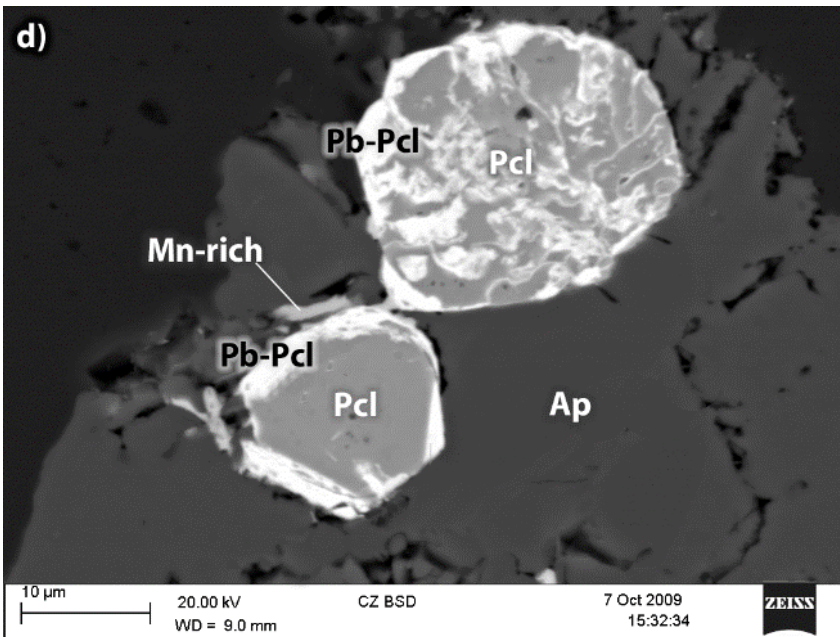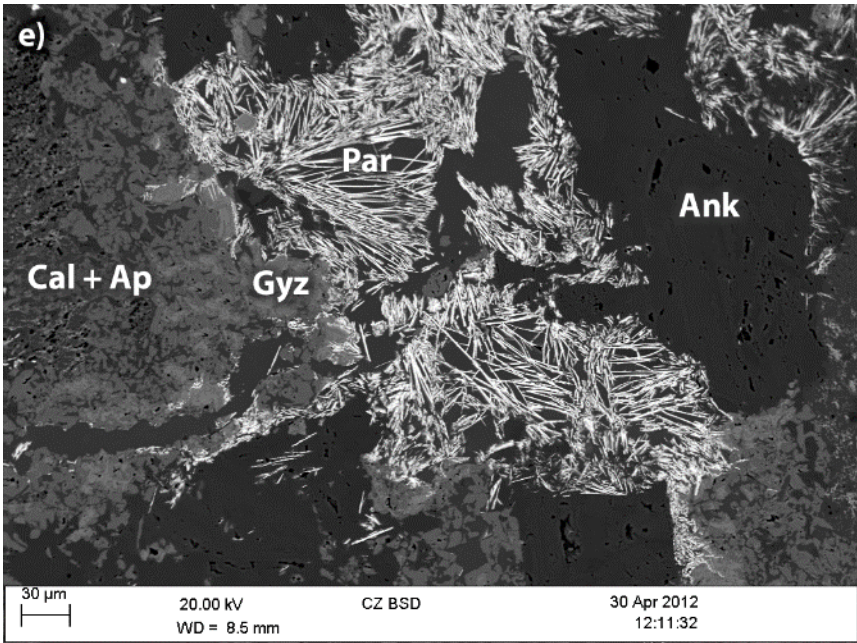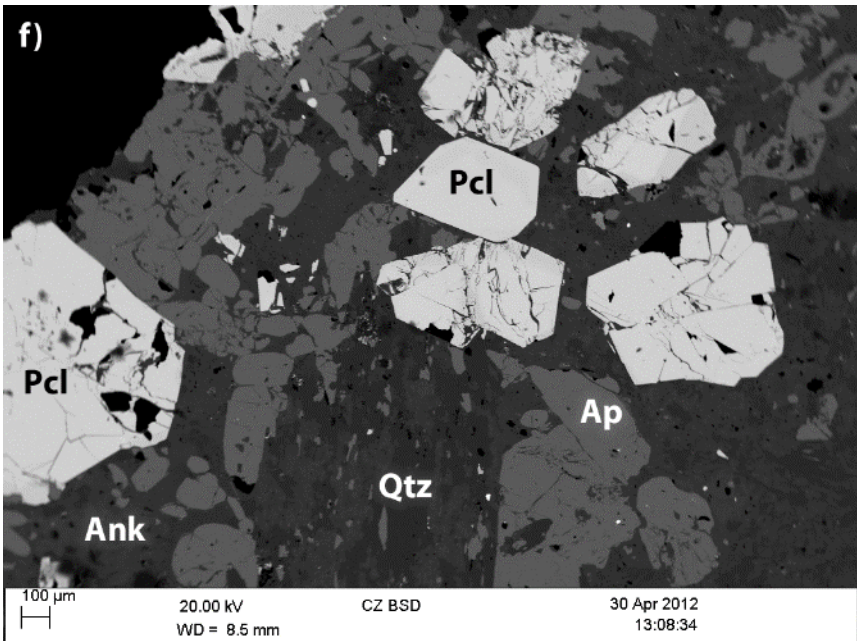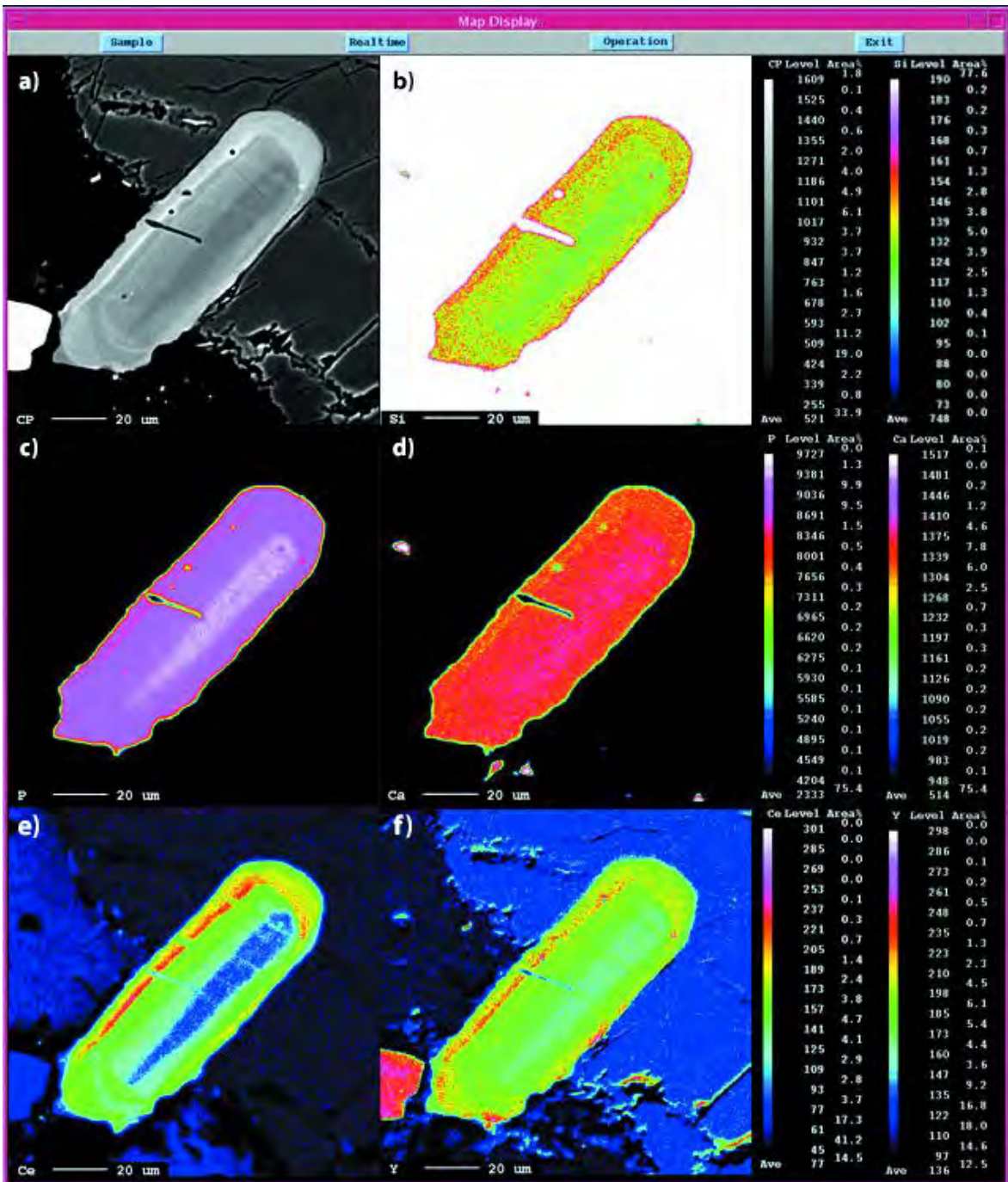
393

394

397

398

399
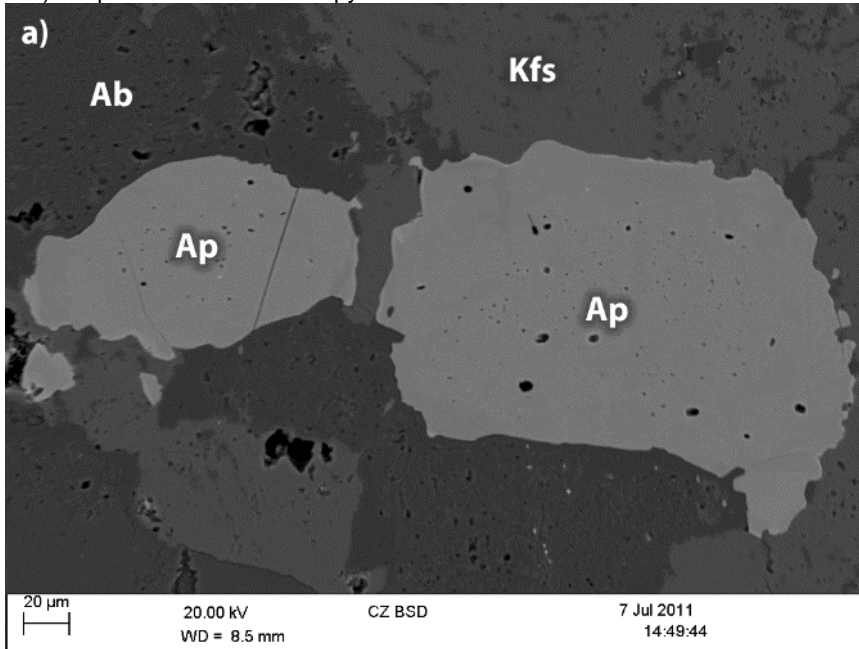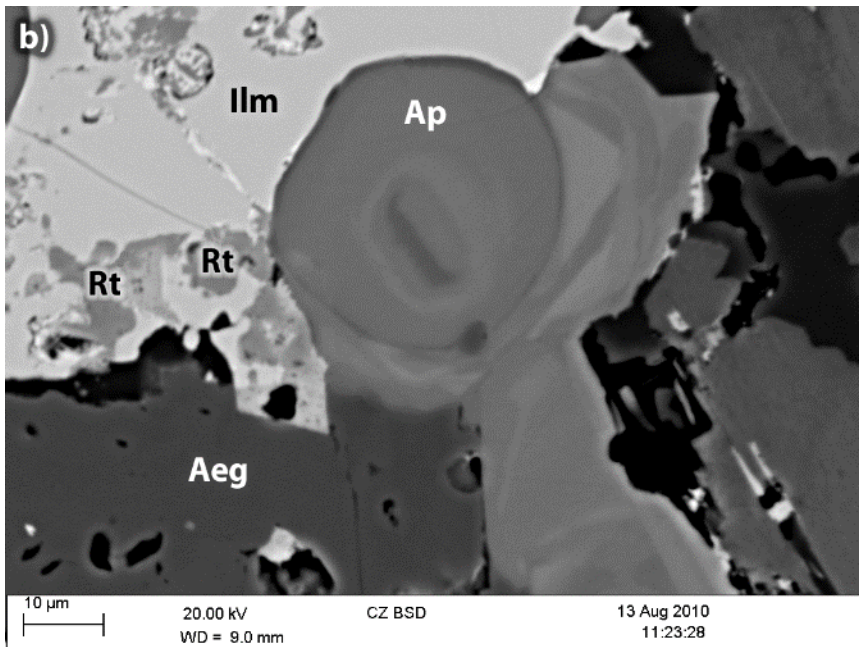
400 **Fig. 6** Element maps of strongly zoned apatite in medium-grade fenite BM1968 P37 78.
401 a) BSE image b) Si   c) P d) Ca e) Ce f) Y   (Na not shown as no zoning evident)
402
403

404

REE patterns in apatite in medium-grade fenite and in carbonatite

Laser ablation analysis of apatite (Table 3) was undertaken to enable a comparison of the REE chemistry of apatite in medium-grade fenite with that of apatite from sövite and ankeritic carbonatite. Mean chondrite-normalised laser ablation data are shown in Figure 7.

Apatite zoning and changes in fluid composition

Apatite zoning, visible under both back-scattered electron imaging and under cathodoluminescence imaging, is most developed in medium-grade fenite, but also occurs occasionally in carbonatite. Zoning in apatite is common, and is thought to result from temporal changes in the environment during crystal growth (Waychunas, 2002) in pulses of metasomatic fluids (Rae et al., 1996; Coulson and Chambers, 1996).

Zoning in apatite at Chilwa Island reflects varying REE content, with zones enriched in the REE being depleted in Ca and P, suggesting an exchange between these elements. Metasomatic alteration of minerals occurs in the majority of cases by coupled dissolution-reprecipitation (Hetherington et al., 2010). The structure and chemistry of apatite allow for numerous substitutions (Hughes and Rakovan, 2002), but Harlov and Förster, and references therein, (2003) note that the two main coupled cation substitutions involving the REE are:

$$Si^{4+} + (Y+REE)^{3+} = P^{5+} + Ca^{2+}$$
$$Na^+ + (Y+REE)^{3+} = 2Ca^{2+}$$
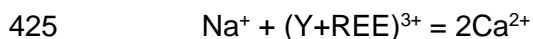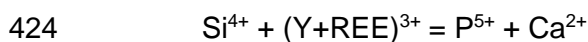
The element maps (Figure 6) indicate that, despite the sodic alteration of the fenite, the more likely substitution in Chilwa Island fenitic apatite involves Si rather than Na. Monazite inclusions as rim grains in apatite are also likely to have been formed by this process (Harlov and Förster, 2003), and postdate apatite. In BM1968 P37 83, monazite is formed where apatite has become porous.

Fenite apatite contains a distinct negative Eu anomaly, which persists on normalisation to the host rock (Figure 7, Table 4). However, several factors combine to make an inheritance of the anomaly from a possible basement origin of apatite unlikely. Sövite at Chilwa Island contains abundant apatite, and thus the surrounding metasomatic environment is favourable for apatite formation. The apatite geochemical data can be interpreted using the classification and regression trees (CART) of Belousova et al., (2002) to assign the host rock from which the apatite derived. Results suggested a larvikite (syenitic) or jacupirangite (pyroxenitic) rather than a granitic host. The cathodoluminescence colour of granitic apatite is typically yellow to orange (Kempe and Götze, 2002) rather than the violets seen in fenite

442   apatite. At Chilwa Island, the presence of apatite in assemblages of other metasomatic

443   minerals in fenite, its RE-zoning and monazite inclusions all indicate a carbonatite

444   association.

445

446   Rather than being inherited, the Eu anomaly suggests the presence of Eu^{2+} and therefore

447   a more reducing environment either at, or before, the time of apatite crystallisation, with

448   Eu^{2+} being preferentially partitioned into an alternative mineral. Under oxidising conditions,

449   because Eu^{3+} would be expected to behave in a similar way to Sm and Gd, REE

450   fractionation would not occur. However, this explanation needs to be compatible with the

451   evidence for the existence of oxidising conditions at Chilwa Island. This evidence includes

452   firstly, the purple cathodoluminescence of fenite apatite, which is attributed to Eu^{3+}

453   activation compared to the blue luminescence seen in apatite from carbonatite, which is

454   related to Eu^{2+} (Mariano and Ring, 1975; Hayward and Jones, 1991; Portnov and Gorobets,

455   1969; Voron'ko et al., 1992). Secondly the redox effect of the alkali content of liquids (Markl

456   et al., 2010) does not appear to be applicable to Chilwa Island. This is associated with

457   closed systems of predominantly sodic nature in quartz-absent rocks, where crystallisation

458   of minerals incorporating ferric iron, such as aegirine or arfvedsonite, leads to reduction of

459   the residual fluid. At Chilwa Island, rocks are not quartz-poor, and aegirine formation was

460   followed by ferric amphiboles, and we thus infer that oxidised fluids continued to enter the

461   aureole via the open system pertaining at the complex. Thirdly, Eu is thought to be

462   predominantly in the trivalent state in relatively low temperature hydrothermal fluids below

463   250˚C (Sverjensky, 1984), which may be typical of the fenite environment in the less

464   intensely metasomatised parts of the aureole.

465

466   At Chilwa Island, the sequence of fluids is thought to have become increasingly oxidised

467   over time. The favoured explanation for the negative Eu anomaly is that apatite formed

468   relatively early in this sequence. Eu^{2+} was partitioned into earlier, and probably also

469   contemporaneous, minerals. Plagioclase and K-feldspar take up Eu more readily than other

470   REEs, leading to negative Eu anomalies in co-existing phases (Leeman and Phelps, 1981).

471   It is believed that at Chilwa Island, early alkaline fluids generated from sövite magma would

472   have precipitated plagioclase and limited amounts of K-feldspar, with a possible later

473   expulsion of potassic fluids producing further K-feldspar. The attribution of the apatite

474   negative anomaly to mineral crystallisation sequence was tested by plotting Eu/Eu* against

475   Sr in apatite (Dowman, 2014). Sr also partitions preferentially in feldspar, and apatite plots

476   would be expected to demonstrate a relationship between decreasing Sr and a deepening

477   negative Eu anomaly if crystallisation sequence effects were dominant. However, although

478   no clear relationship emerged, both plagioclase and orthoclase at Chilwa Island are known

479 to have pronounced positive Eu anomalies (David Banks personal communication). The
480 precipitation order of minerals is therefore considered the most likely cause of the negative
481 Eu anomaly in apatite.

482

483 Apatite in fenite is equally enriched in LREE, and is more enriched in the HREE than apatite
484 in carbonatite (Figure 7, Table 3). Fenite apatite is also more enriched in all REE than the
485 ankeritic carbonatitic apatite. The trend of relative MREE/HREE fenite enrichment is also
486 seen in other RE-bearing minerals.

487
488 **Table 3** LA-ICP-MS REE in apatite at Chilwa Island (ppm)

| Element	Fenite BM1968 P37 32		Fenite BM1968 P37 78		Fenite BM1968 P37 96		Sövite 1957 1056 59		Ankeritic carbonatite 1957 1056 122	
n = 16*	Average	Std dev	Average	Std dev	Average	Std dev	Average	Std dev	Average	Std dev
Y	1625	894	1553	492	2761	1572	219	27	1367	221
La	2687	1107	3520	1050	1902	939	2592	301	168	56
Ce	5370	2378	6877	1559	4476	1953	5191	565	606	154
Pr	640	301	913	283	708	297	620	66	94	22
Nd	2606	1300	3473	925	3336	1447	2276	242	512	121
Sm	460	250	560	159	726	343	292	33	191	40
Eu	34	16	59	22	71	46	68	7	78	14
Gd	417	234	456	129	687	347	168	19	256	49
Tb	53	30	55	16	91	49	14	1	41	7
Dy	313	175	307	90	543	315	56	6	259	45
Ho	58	32	57	16	102	59	7	1	46	7
Er	147	82	141	41	260	157	12	1	113	19
Tm	18	9	18	6	34	22	1	<1	13	2
Yb	99	53	99	30	198	132	6	1	64	11
Lu	13	6	14	4	27	18	1	<1	7	1

489 * n = 3 for BM1968 P37 78

490

491

492 **Fig. 7** Chondrite-normalised average REEY for apatite in fenite (green) and carbonatite (red/pink) at Chilwa
493 Island. Ank carb = ankeritic carbonatite. Data from LA-ICP-MS. Error bars represent one standard deviation
494
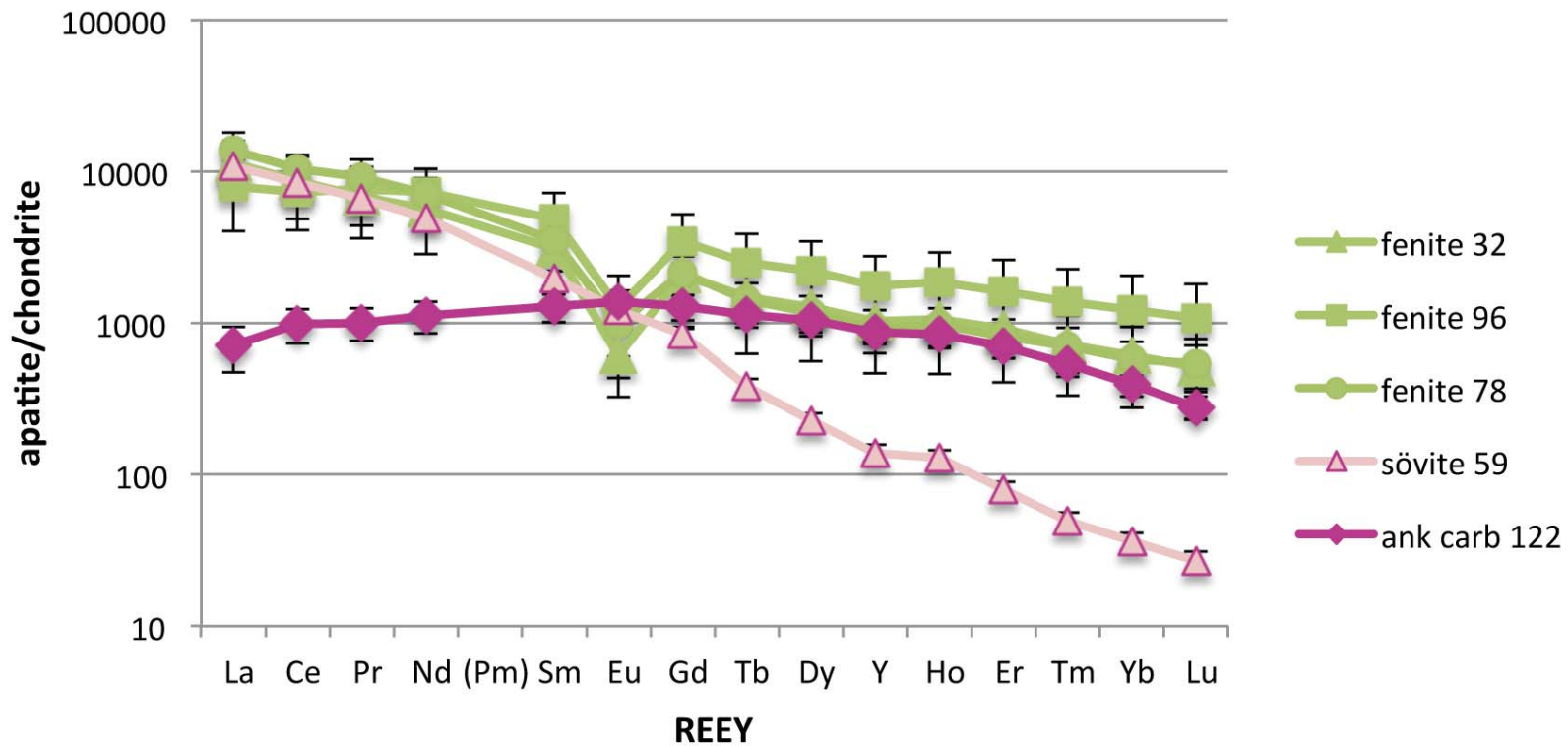
497 **Table 4** Eu/Eu* anomaly at Chilwa Island
498 a) in whole-rock fenite and carbonatite

Low-grade fenite	Medium-grade fenite	Breccia	BM1968 P37 83	Sövite	Ankeritic carbonatite	Sideritic carbonatite
1.03±0.22	0.95±0.05	1.07±0.03	0.97	0.84±0.02	0.88±0.06	0.66±0.02

499
500 b) in apatite in medium-grade fenite, sövite and ankeritic carbonatite

Fenite BM1968 P37 32	Fenite BM1968 P37 96	Fenite BM1968 P37 78	Sövite 1957 1057 59	Ankeritic carbonatite 1957 1056 122
0.25±0.03	0.29±0.04	0.35±0.10	0.86±0.01	1.08±0.01

501

502 **LREE-MREE patterns in monazite, bastnäsite and parisite**

503 EDS analyses of LREE to MREE patterns of monazite, bastnäsite and parisite are shown
504 in Figure. 8. The fenite minerals all show higher MREE/LREE ratios compared to their
505 carbonatitic counterparts. This is particularly notable in the mid REE-enrichment in minerals
506 of the high-grade, quartz-rich rock, BM1968 P37 83.

507

508 **REE variation in minerals in carbonatite and in fenite**

509 In general, the LREE enrichment of carbonatites is reflected in the composition of their RE-
510 bearing minerals, although considerable variation in REE distribution in minerals occurs at
511 many complexes (Smith et al., 2000; Zaitsev et al., 1998, Bühn et al., 2001; Cooper and
512 Paterson, 2008). At Chilwa Island, the RE-bearing minerals in fenite all have lower La/Nd
513 ratios than their carbonatitic equivalents. This is also true for the RE-rich carbonatite
514 complex of Kangankunde in Malawi (Dowman, 2014).

515

516 Variations in REE profiles may result from a number of factors. Firstly, carbonatite
517 fractionation from Ca-rich to more Fe/Mg- and fluid-rich compositions may drive down La/Nd
518 ratios in minerals (Bühn et al., 2001; Cooper and Paterson and citations therein. 2008;
519 Drüppel et al., 2005). The carbonatite sequence at Chilwa Island indicates this could be a
520 relevant factor.

521

522 Another factor to be considered is that the precipitation order of minerals is intricately linked
523 to carbonatite fractionation (Hogarth, 1989; Woolley and Kempe, 1989; Le Bas, 1999; Bühn,
524 2008). Early LREE-rich crystallising phases such as allanite and monazite may cause a
525 flatter REE profile in later minerals such as apatite (Hoskin et al., 2000; Miles et al., 2013).
526 This factor is discounted at Chilwa Island as no allanite was identified in any section, and
527 the expected Nd anomalies are not present in monazite. Furthermore, it is thought that
528 monazite crystallised later than apatite and would therefore have played no role in
529 determining apatite composition.

530

531   A third factor is that hotter, CO_2-rich fluids may promote La-enrichment of minerals, with

532   lower La/Nd mineral ratios resulting from dominantly aqueous fluids of lower temperature

533   (Smith et al., 1999; 2000; Zaitsev et al., 1998). Evidence from fluid inclusions at Chilwa

534   Island was insufficient to establish the existence of this relationship.

535

536   A brief examination of the role of ligands notes that the transportation of the REE in fluids

537   is thought to be facilitated by their binding to a variety of ligands to form co-ordination

538   complexes of different stability (Gieré, 1996). Suggested ligands include Br^-, Cl^-, NO_3^-, OH^-

539   and F^-, as well as $P_2O_5^{2-}$, SO_4^{2-} and CO_3^{2-}. The stability of the REE with these ligands is

540   contentious and is a continuing area of active research. F is common at Chilwa Island as

541   evidence by the presence of fluorapatite and F-rich RE-carbonate minerals, and was

542   previously thought likely to be a key ligand operating to complex the REE and Th (Keppler

543   and Wyllie, 1990; Finch, 1995; Goodenough et al., 2000; McCreath et al., 2012). The

544   effectiveness of fluoride complexes, compared to chloride and sulphate complexes, as

545   agents of REE transport is now being questioned (Migdisov and Williams-Jones, 2014), and

546   F may act more as a binding ligand that promotes REE deposition, particularly where fluid

547   interacts with host rocks of a higher pH. At Chilwa Island, this could have occurred when

548   feldspar-bearing rocks buffered the hydrothermal fluids expelled from the carbonatite.

549   However, at Chilwa Island, sulphate complexes are not important, and the role of Cl is

550   undetermined, but Cl was not detected in fluid inclusions analysed by laser ablation ICP-

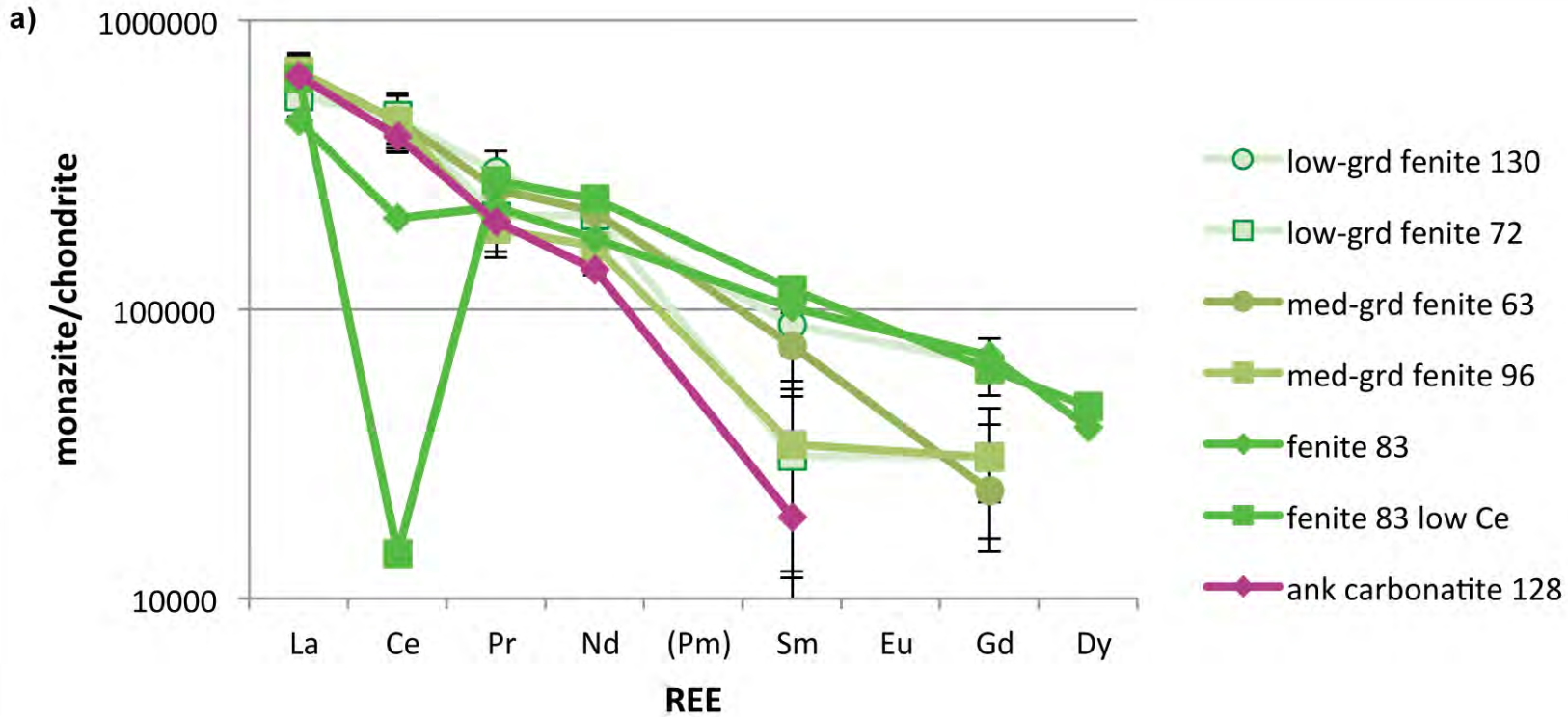551   MS (David Banks, personal communication).

552
553
554
555 **Fig. 8** Chondrite-normalised LREE in minerals in fenite (green) and carbonatite (red/pink) at Chilwa Island
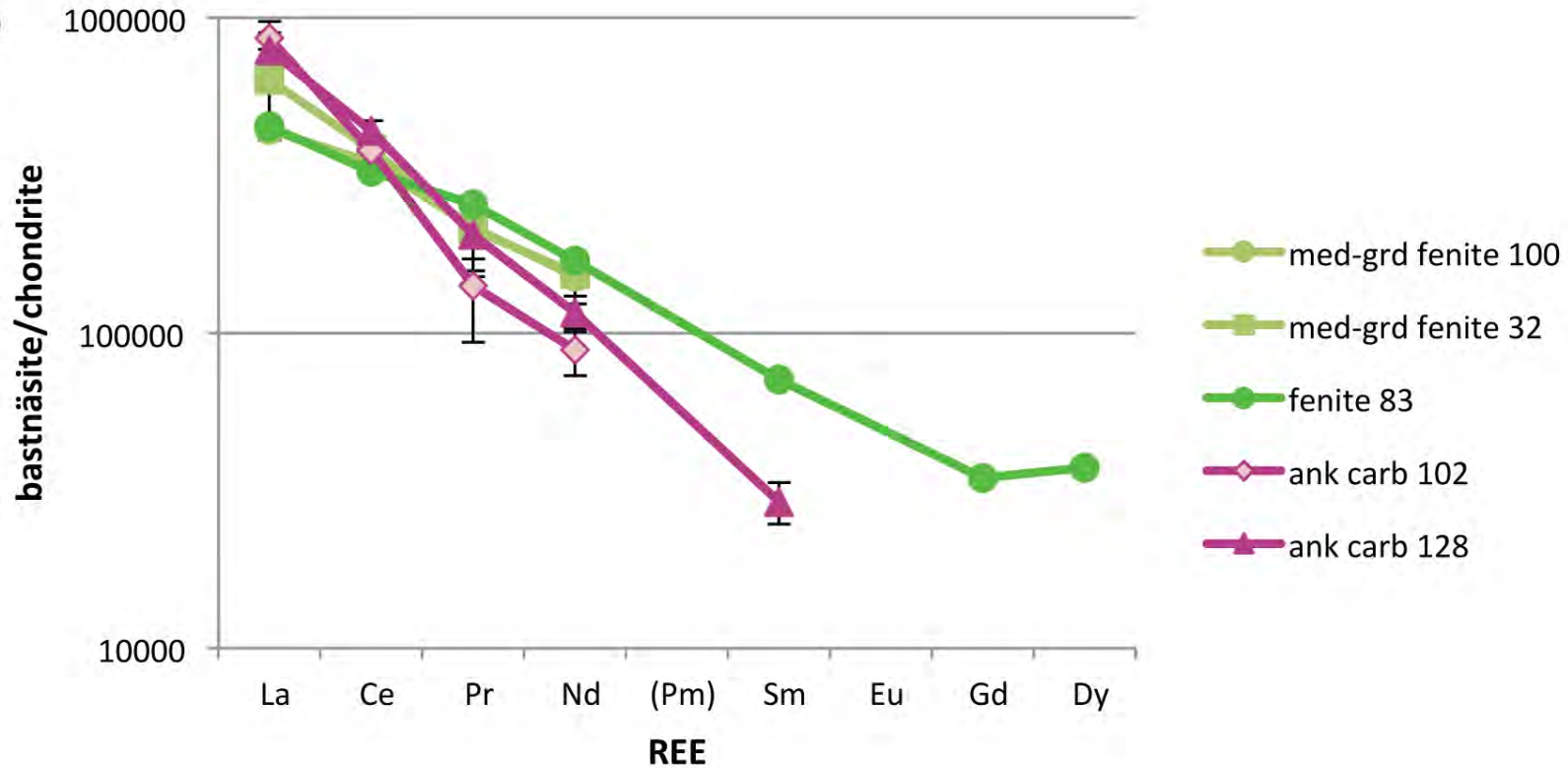556   a) monazite   b) bastnäsite   c) parisite
557 Data from EDS. Error bars represent one standard deviation. Fenite 83 monazites are individual analyses
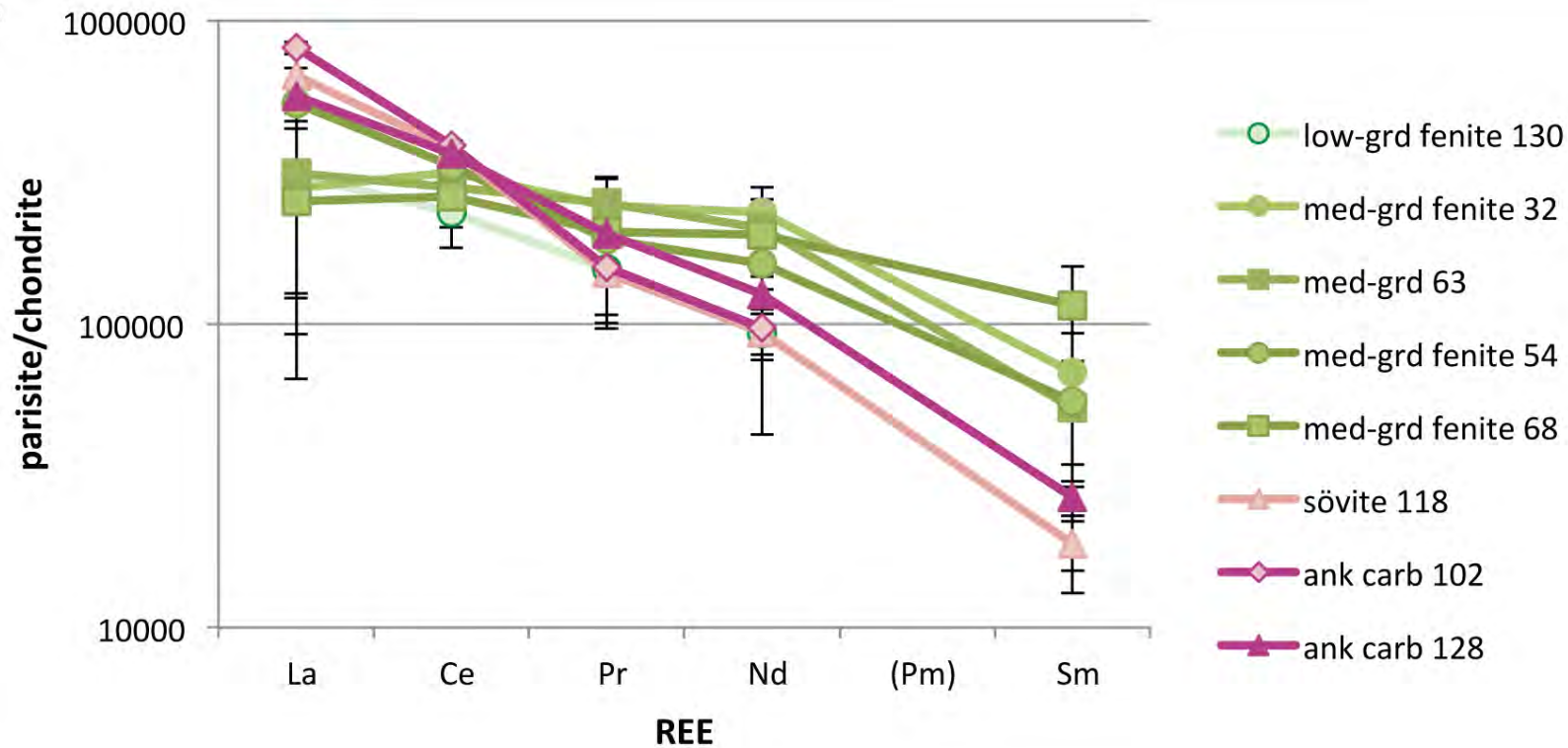558

a)

b)

c)

Whole-rock chemistry

Tables of results are included in supplementary information.

Major elements

As expected from the mineralogical variations across the fenite aureole, the major element data also indicate that the fenite samples fall into discrete groups, although without any obvious subdivision of the medium-grade group. Some unexpected similarities exist between the low-grade fenites and breccia, which given the spatial separation of these groups in the aureole, might have been expected to exhibit the strongest contrasts. Both groups have a low Fe, Mg, Mn and Ti content compared to the medium-group fenite (Figure 3b).

Apart from the quartz rock BM1968 P37 83, which is devoid of alkalis, total alkali content is similar across fenite grades, but this masks a change from the strongly potassic breccia adjacent to the carbonatite to the outer fenite zones where levels of Na and K are similar (Figure 3b).

Trace elements

Among the trace elements, a similarity of pattern of enrichment and depletion exists between carbonatite and fenite, with enrichment in Ba, Mo, Nb, Pb, Sr, Th and Y and depletion in Co, Hf and V. Enrichment in carbonatitic type elements generally increases towards the inner parts of the aureole (Figure 3c). Fenite normalisations to the series sövite, ankeritic carbonatite and sideritic carbonatite revealed a sequence of increasing differences in element concentration between fenite and carbonatite (Dowman, 2014).
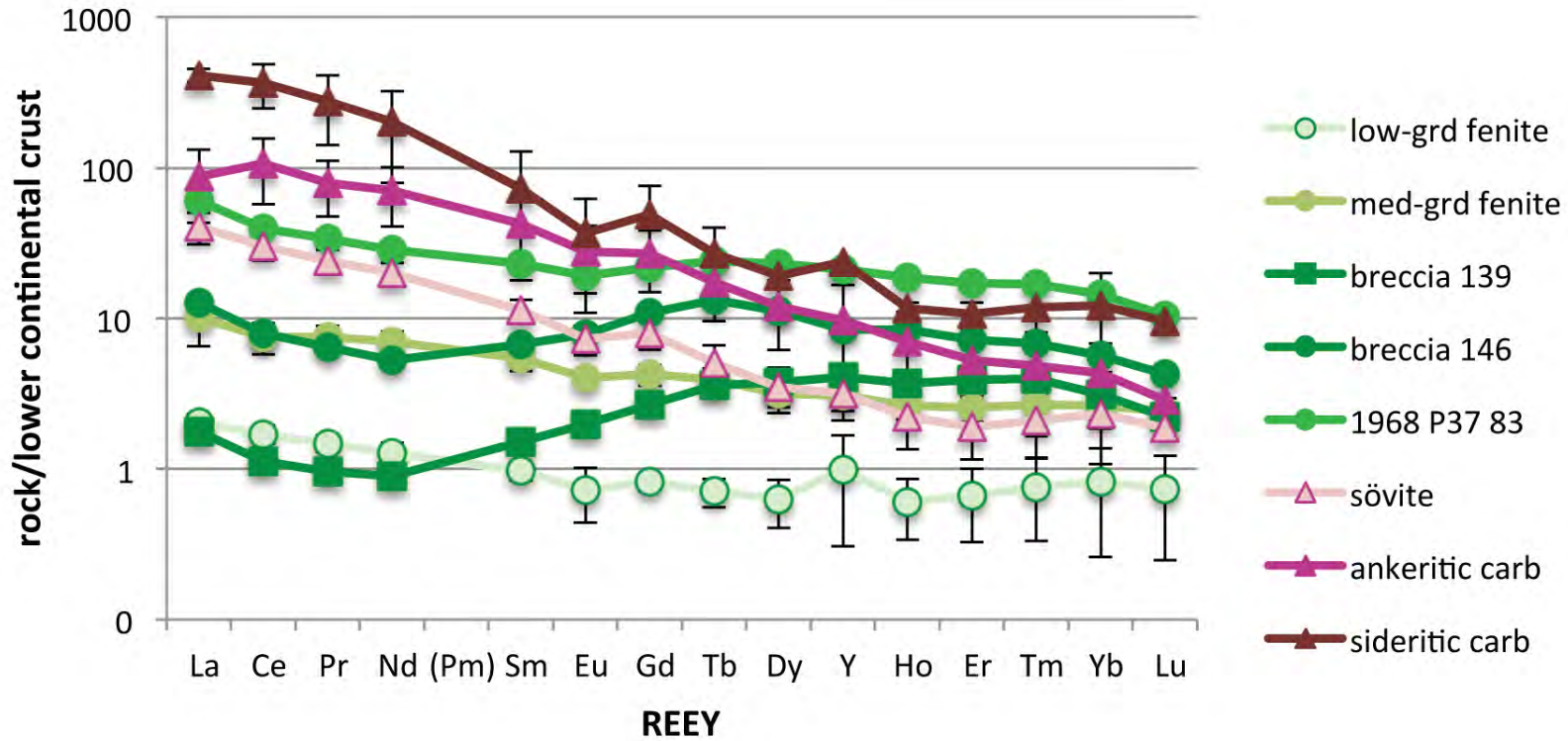
REE

Normalisation of the REE to average lower continental crust, which is taken as a proxy for country rock, shows the fenite profiles to be flatter than those of the carbonatites (Figure 9, also see chondrite normalisations in Table 5). Carbonatites are relatively LREE-enriched, and the HREE content of breccia and the main (medium-grade) fenite group is higher than that of sövite, and similar to that of ankerite. The most altered rocks display distinctive profiles. BM1968 P37 83 has higher levels of the REE from Dy to Lu than any of the averaged results for carbonatite in the complex, and the highest level of Ho and Er of any of the rocks analysed. The unusual profiles of the two breccia samples show a rising trend from Nd to Tb, with relatively high levels of the HREE. Fenite Eu anomalies are generally smaller than those of carbonatites, and may be either mildly positive or negative. No clear difference in anomalies exists between fenite groups, but carbonatites show increasing negative anomalies in the sequence sövite-ankeritic carbonatite-sideritic carbonatite (Table 4a).

595

596   **Fig. 9** Lower continental crust-normalised rare earth elements for average fenite grades (green) and
597   carbonatites (red/pink) at Chilwa Island. Error bars represent one standard deviation
598

Legend:
- low-grd fenite
- med-grd fenite
- breccia 139
- breccia 146
- 1968 P37 83
- sövite
- ankeritic carb
- sideritic carb

Y-axis: rock/lower continental crust

X-axis: REEY (La, Ce, Pr, Nd, (Pm), Sm, Eu, Gd, Tb, Dy, Y, Ho, Er, Tm, Yb, Lu)

599

600 **Table 5** Chondrite-normalised La/Yb ratio for fenites and carbonatites at Chilwa Island

| Rock Ratio	Low-grade fenite	Medium-grade fenite	Breccia	BM1968 P37 83	Sövite	Ankerite	Siderite
La/Yb	6.7-16.0	8.5-26.9	2.0-8.2	15.1	48-220	27-164	78-240

601

Fluid inclusion data

603 Examination under the optical microscope showed that quartz is the most important host
604 for inclusions. Feldspar is also a common matrix mineral, but is highly altered and does not
605 contain easily identifiable inclusions. Quartz is not common in more altered fenite, and when
606 present, is generally recrystallised and without fluid inclusions. The investigation was
607 therefore restricted to lower-grade fenite. The inclusions found in the low- and medium-
608 grade fenite are typically a few µm in diameter, secondary in nature and extremely
609 heterogeneous. Among the larger inclusions, single phase, 2- and 3-phase, single solid and
610 multi solid-bearing examples are present, with 2-phase being the most abundant, and single
611 phase also common (Figure 10). Little change in the proportions of different inclusion types
612 was found between low- and medium-grade fenite beyond a small increase in the number
613 of solid-bearing inclusions found in medium-grade fenite. Inclusions are often found in
614 crosscutting trails, but were too small to allow characteristics of particular trails to be
615 distinguished. CL imaging of quartz grains revealed a low-luminescent network of fractures
616 coinciding spatially with the inclusion trails (Dowman, 2014).

617

618

619

620 **Fig. 10** Sketch of typical fluid inclusion trails found in quartz of low- and medium-grade fenite at Chilwa Island.
621 Enlarged portions illustrate heterogeneity of inclusions

622
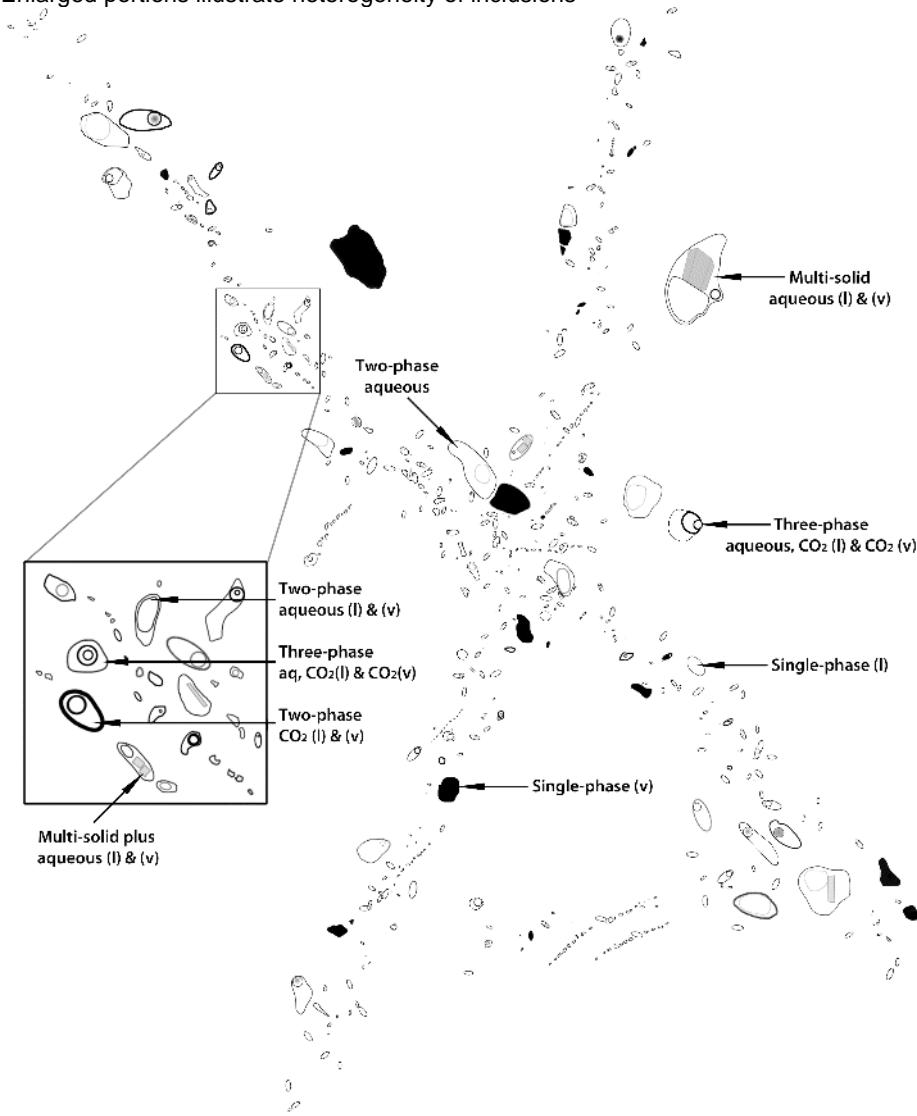
623 Based on Raman analyses, these fluid inclusion assemblages comprise: i) CO_2-rich

624 aqueous fluids with little or no methane and nitrogen, ii) monophase aqueous inclusions,

625 III) liquid and vapour aqueous inclusions and iv) multiphase carbonate-bearing inclusions

626 containing nahcolite and burbankite daughter phases indicative of REE-Ca-H_2O-CO_2

627 compositions. These fluids seems to have followed the same pathways in the quartz as

628 indicated by the CL which could indicate either several pulses of different fluids at different

629 times or heterogeneous trapping of mixed or unmixed pulses of fluid. A combination of both

630 seems most likely.

631

632 Microthermometric measurements were hampered by decrepitation of inclusions at around

633 200˚C before total homogenisation occurred, but data relating to the melting temperature

634 of CO_2 clustered close to the triple point of -56.6˚C, indicating the inclusions contain

635 relatively pure CO_2 and little of other volatiles such as CH_4 and N_2, which depress melting
636 points. Partial homogenisation of the CO_2 phase was always to the liquid phase at
637 temperatures between 0.3 and 30.2˚C, corresponding to CO_2 densities of ~0.9 to 0.6g/cm^3.
638 No systematic relationship could be determined between homogenisation temperature and
639 CO_2 fill.
640
641 Whether these fluids were also chloride-rich is unresolved because halite (NaCl), though
642 tentatively identified optically, if present, is Raman inactive. Also, although Cl was not
643 detected by ICP-MS analysis of the fluid inclusions (David Banks, personal communication),
644 this is at variance with microthermometric data for frozen inclusions. These showed first
645 melting temperatures of frozen inclusions commonly occurred at around -24˚C, which is
646 close to the eutectic temperatures for both $NaCl-H_2O$ and $NaHCO_3-H_2O$ systems (Shepherd
647 et al., 1985). Unfortunately, final melting temperatures could not be recorded with any
648 degree of accuracy to determine total salinities.
649

Towards a model for metasomatism in fenite at Chilwa Island

The main purpose of this paper is to develop a model to enable characterisation of the metasomatic fluids that caused wall rock fenitisation at Chilwa Island. In order to do this, certain aspects of magmatic fluids need to be briefly addressed.

Firstly, fluid expulsion from magma is unlikely to constitute a single event (Verschure and Maijer, 2005). At Chilwa Island, it is highly likely that multiple fluids were generated. The complex is thus the result of a number of episodes of magma emplacement, each of different composition, each of which would have produced associated fluids.

Secondly, two processes can lead to oversaturation of the key volatiles, water and carbon dioxide, with subsequent magma boiling and the expulsion of fluids. A 'first boiling' can result from a decrease in pressure during magma ascent (Candela, 1997). Fluids lost by a carbonatite in this way may be predominantly alkaline, and thus be responsible for fenitisation (Wall, 2000). 'Second boilings' occur isobarically when crystallisation of anhydrous phases concentrates volatiles in the remaining melt. The fluids subsequently expelled may be more mineralising in nature, carrying and precipitating elements such as Ca, Fe, Zn and the REE (Drüppel et al., 2005; Gieré ,1996; Brimhall and Crerar, 1987). As melts may also undergo a series of crystallisation episodes, volatile saturation would therefore be a 'quasi-periodic process' (Candela and Brevin, 1995), resulting in multiple associated fluid expulsions from each magma.

Thirdly, with reference to the relative importance of the role played by the two key volatiles in magma saturation, it is recognised that carbonatite-derived fluids can have very variable CO_2/H_2O ratios, with CO_2 not always dominant (Drüppel et al., 2005). CO_2 saturation may also occur independently of H_2O fluid saturation (Robb, 2009; Keppler, 2003). However, as discussed above in relation to REE ratios, hotter fluids (proximal to the carbonatite) may be CO_2-rich compared to cooler, and more aqueous, distal fluids. In the outer parts of the aureole at Chilwa Island, the fluid inclusion evidence shows that both volatiles are present, but because there is no clear pattern or trend in their distribution, their relative importance here is not determined.

On the basis of the field and laboratory data outlined above, it is possible to propose a robust model for fenitisation at Chilwa Island that involves a sequence of magmatically derived fluids (Figure 11). This data supporting the presence of multiple fluids include the presence of a sequence of carbonatites, each likely to have generated fluids, as well as evidence of the variation in spatial distribution of mineral assemblages, the zonation in

687   apatite, the contrasts in zircon habit, the existence of high-grade fenites with differing
688   monophase matrices, and the heterogeneity of fluid inclusions. Thus, in the model, these
689   fluids are related to a succession of magma emplacement events starting with sövite, then
690   ankerite and finally siderite. Figure 12 provides a suggested paragenetic sequence for the
691   formation of minerals associated with carbonatite emplacement and the fenitisation process.
692

a) Sövite growth/emplacement

Pervasive sodic-dominant fenitisation either
contemporaneous with or pre intrusion
emplacement

b) Ankerite growth/emplacement
Intrusion of carbonatite associated with
multiple episodes of mineralisation along
veins and fractures
Increasing oxidisation of fluids, and
fractionation of REEs

**c) Late ankerite growth/emplacement to
pre siderite growth/emplacement**
Potassic fluid of limited extent, associated
with further brecciation, pervasive in nature
proximal to carbonatite and directed along
vein and fracture network more distally.
Zr mobilisation?

d) Siderite growth/emplacement
Limited mineralisation along veins and
fractures
Late-stage hydrothermal circulation
remobilises silica

**e) Complex after cessation of magmatic
and hydrothermal activity**

Fig. 11 Schematic model for fluid sequence affecting fenite rocks at Chilwa Island

KEY: L: Low-grade fenite
          M: Medium-grade fenite
          MH: Medium/high-grade fenite
          FB: Feldspathic breccia
          C: Carbonatite
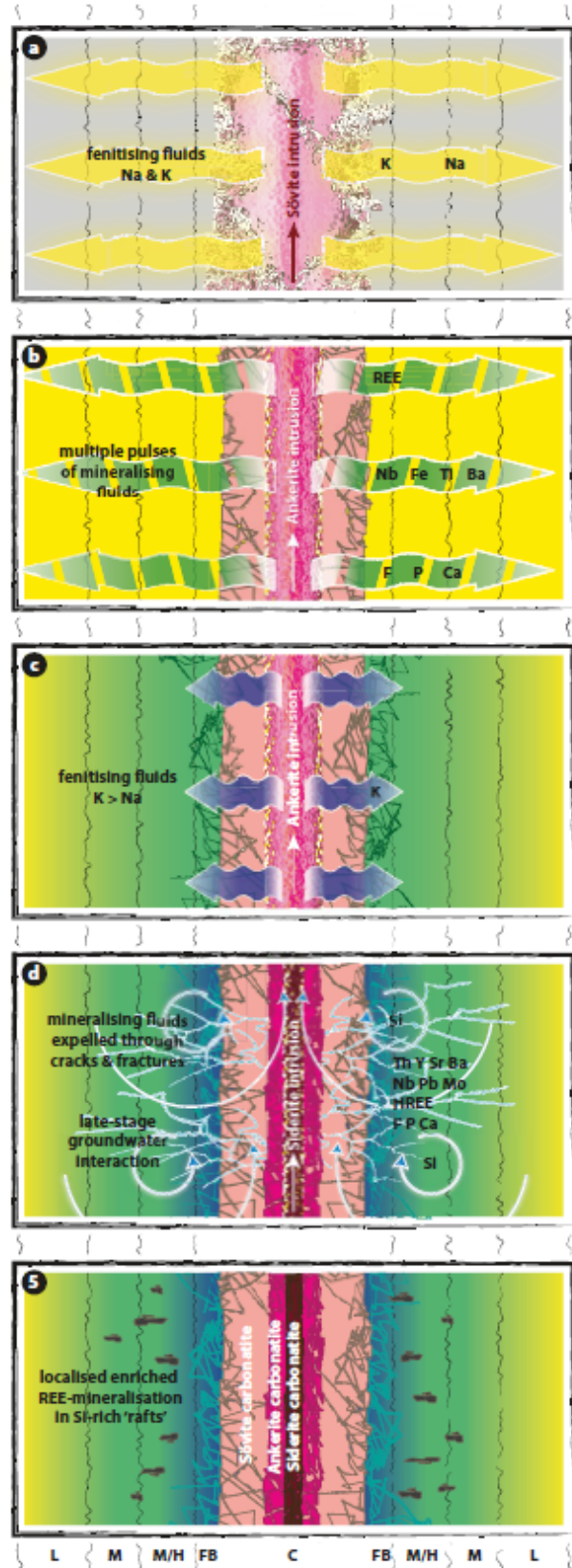
a) Early fluids, associated with sövite

The first fenitising fluids were predominantly sodic, and were expelled before or during intrusion of the sövite, probably as a result of decompression-driven first magma boiling (Figure 11a). This is consistent with field data that show plagioclase is present as a matrix material in all low- and medium-grade fenite samples. It also concurs with previous research indicating that sodic fluids are often expelled at an early stage of emplacement of carbonatite complexes (Le Bas, 1977; 2008; Drüppel et al., 2005; McKie, 1966; Vartiainen and Woolley, 1976; Woolley, 1982). This fluid event was spatially more extensive than later events and its extent was probably facilitated by the brecciation, widespread at Chilwa Island, which typically accompanies carbonatite emplacement (Le Bas, 1987). Similar levels of Na in the aureole from medium-grade fenite outwards suggest a pervasive fluid, which altered country rock across the island. On a micro-scale, the inward-spreading turbidity in feldspar grain margins, as described above in the mineralogy of medium-grade fenite, indicates that crystal boundaries formed channels for fluid migration, similar to that seen in quartz under CL imaging (Dowman, 2014). Further migration of fluids may have been facilitated by microporosity of mineral grains (Finch and Walker, 1991).

The sövitic magma may also have experienced a second boiling linked to isobaric crystallisation. However, compared to the ankeritic and sideritic carbonatites, the composition of the sövite is low in Fe, the REE and other typical carbonatitic elements such as Ba, Nb and Y. Therefore, if a second boiling did occur, and these elements were mobilised into the expelled fluids, they would have been at concentrations too low to form the source of the ilmenite and aegirine mineralisation seen in the fenite rocks. The vestiges of any second boiling event would have been largely lost due to subsequent overprinting by fluids from the younger carbonatites. The apatite in the fenite provides the strongest evidence for the existence of this second stage fluid. Sövite at Chilwa Island contains apatite, and is the carbonatite richest in Ca and P. Apatite growth in fenite has been dated (Dowman, 2014) as contemporaneous with carbonatite emplacement, and any fluid arising from a second boiling would have mobilised these elements out into the fenite rocks, where they were precipitated to form the RE-poor cores (Figure 6) of the apatite grains commonly seen in medium-grade fenite.

b) Fluids associated with ankeritic carbonatites

The emplacement of this carbonatite may have been accompanied by an early expulsion of alkali fluids. However, any evidence of a first boiling has been lost among the effects on the aureole from the preceding sövite-related alkali-rich fluid event.

773   Mineralogical data reported here suggest that a punctuated second boiling event occurred
774   (Figure 11b). This was probably caused by periodic recharge of the magma body as part of
775   an open system (Norton and Pinkerton, 1997). Anhydrous minerals, such as apatite,
776   probably crystallised in successive stages, resulting in the expulsion of fluids as a series of
777   pulses.

778

779   Although this fluid event appears to have been more restricted in extent that that associated
780   with the expulsion of the alkaline sövitic fluids, it was probably the main mineralising event
781   as fluids predominantly transported the REE, together with Nb, Ti, Fe, Ba, P and Ca, rather
782   than the alkalis, into the aureole. The RE-bearing mineral, burbankite, identified in fluid
783   inclusions (Dowman, 2014), provides direct evidence that REE were mobilised in fluids from
784   the carbonatite at this stage. The extensive aegirine mineralisation of the aureole is also
785   associated with this episode, and is most likely the result of precipitation of Fe carried in the
786   fluids, together with remobilisation of Na from plagioclase.

787

788   Mineralisation is focused chiefly into veins and fractures, suggesting possible structural
789   control along pre-existing lines of weakness. This is supported by the spatial distribution of
790   zircons of Pan African age in these veins (Dowman, 2014) that appear to have acted as
791   nuclei for the characteristic micro-mineral assemblages of Nb-bearing ilmenite and
792   fluorapatite with monazite inclusions that are present in medium-grade fenite rocks. The
793   inference is that carbonatite emplacement may have reactivated earlier tectonic fluid
794   pathways.

795

796   Evidence of multiple fluid ingress, with a changing fluid composition, is reflected in REE
797   zoning in apatite in medium-grade fenite (Figure 5b), and perhaps also in the zoning in the
798   outer parts of some apatite grains in the earlier sövite (Dowman, 2014). Fission-track dating
799   of apatite in fenite (Dowman, 2014) established that it is contemporaneous with apatite
800   found in a nepheline-syenite plug of carbonatite age at Chilwa Island (Eby et al., 1995).

801

802   **c) Late-stage ankerite emplacement to pre-siderite emplacement**
803   A strongly potassic fluid event is associated with a possible first boiling of fluids enriched in
804   CO_2 (Rubie and Gunter, 1983) during the phase of late ankerite/pre-siderite emplacement.
805   This caused a further brecciation episode as well as fracturing of the high-grade fenite of
806   the inner aureole (Figure 11c). Potassic fenite may be produced from magma at higher
807   levels in carbonatite complexes (Le Bas, 2008; Viladkar, 2012) and associating K-
808   fenitisation with relatively late-stage magma here would be compatible with the evolution of
809   the Chilwa Island complex, where the carbonatite emplacement sequence of sövite,

810 ankerite and siderite is believed to have occurred at successively higher levels (Garson and
811 Campbell Smith, 1958).

813 Compared to the earlier sodic alkaline fluids, this fluid was spatially restricted in its effect.
814 However, it pervasively altered the breccia, and caused K-feldspar enrichment of the
815 high/medium-grade fenite. Dissolution of zircon in both these zones probably occurred after
816 reaction with this caustic potassic fluid. Zr can become highly mobile in F-rich alkaline fluids
817 (Rubin et al., 1993), and at Chilwa Island, evidence of this can be seen in the reprecipitation
818 of Zr as nano-sized zircon grains occasionally found in apatite (Dowman, 2014). Further out
819 in the aureole, the potassic fluid caused limited alteration along mineral veins. CL imaging
820 revealed potassic feldspar surrounding etched apatite grains (Dowman, 2014). Within the
821 carbonatites, metasomatism by this fluid formed the K-feldspar found in both ankeritic
822 carbonatite and in sövite.

824 Mineralisation effects from any second magma boiling associated with late ankeritic
825 emplacement cannot be distinguished from that caused by fluids derived from the sideritic
826 carbonatite.

828 **d) Late-stage fluids associated with siderite emplacement**
829 Two contrasting late-stage fluids are interpreted here as controlling the final stages of
830 metasomatism at the Chilwa Island complex. The first of these was responsible for
831 significant mineralisation; the second was a silicification event (Figure 11d).

833 *d.1 Mineralising fluid*
834 The last mineralising fluid is probably related to the intrusion of sideritic carbonatite (possibly
835 also a late-stage ankerite), and a second magma boiling. This fluid appears to represent a
836 limited expulsion of carbonate-bearing, and possibly CO_2-rich fluid, documented
837 predominantly as thin veins containing carbonate in all fenite grades and which also carry
838 occasional goyazite and an unidentified Th-rich RE mineral in the breccia. The range of
839 elements carried by the fluid points to the sideritic carbonatite as being the source, as only
840 this carbonatite has a composition sufficiently enriched in elements such as Th, Y, Sr, Pb,
841 Mo, Ba and the REE (including the HREE) to explain the presence of minerals in the fenite
842 such as xenotime and barite.

844 Chemical data from Chilwa Island suggest that the mobilisation and precipitation of the
845 MREE and HREE became more important in fluids exsolved from the later carbonatites, as
846 the aqueous component of the fluids increased and their temperature decreased (Smith et

al., 2000; Andrade et al., 1999). The hydrothermal origin of barite is in accord with Garson and Campbell Smith's view (1958) when he noted the association of barite with late-stage veinlets. Barite is also present in each carbonatite examined in this study. Xenotime was seen in one carbonatite, the high-grade fenite rock BM1968 P37 83, and as a scarce phase across the fenite aureole out to low-grade fenite. Xenotime is also considered to be a late-stage hydrothermal mineral, possibly being formed at low temperature, via a dissolution-reprecipitation process during fluid-induced alteration of apatite (Harlov, 2011). Cooler temperatures during the waning, more aqueous phase of mineralising fluid episodes may be linked to the formation of the low temperature amphibole, riebeckite. Fractionation of the REE in these siderite-ankerite-derived fluids is suggested by the fall in Nd/Ho ratios from 170-370 in siderite at Chilwa Island to those found in fenite. The high-grade fenite areas (breccia and the quartz-rich rock), most affected by late-stage carbonatitic fluids, have Nd/Ho ratios of between 4 and 24, substantially lower than the ratios of 30-60 for fenite little influenced by this type of fluid. These ratios provide evidence that fractionated carbonatites can lose HREE into fluids driven off from the magma, and thus become relatively depleted in the HREE compared to the LREE, and may explain the MREE-HREE enrichment of fenite RE-bearing minerals compared to their carbonatitic equivalents (Figures 7 and 8). Bühn (2008) proposed a similar process.

Certain parts of the more distal regions of the aureole, as represented by rock BM1968 P37 83, appear particularly enriched in the HREE and Th. In fact, this sample contains more Ho and Er than any other rock analysed, carbonatites included (Figure 9). This may indicate that high-grade quartz-rich areas escaped the purging effects of the earlier, highly potassic fluid, which stripped the breccia in the inner aureole of any pre-existing more LREE-enriched minerals. This pattern of fluid distribution would explain the unusual whole-rock REE composition of the breccia (metasomatised by both potassic and mineralising fluids) and in the quartz-rich rock BM1968 P37 83 (metasomatised by mineralising fluids, but not by the potassic fluid).

That fluids from ankeritic and sideritic carbonatite were probably oxidising in nature can also help to explain, ilmenite mineral separation and the presence of two monazite phases.

Firstly, fluids expelled from siderite carbonatite at Chilwa Island are derived from a rock that is thought likely to have formed during a period of oxidation (Garson and Campbell Smith, 1958). Woolley, (2001) described it as secondary in nature, being almost entirely replaced by iron and manganese oxides, and the brief examination of the siderite carbonatite in this study confirmed the presence of these oxides.

884

885   Secondly, the separation out of magnetite and rutile within the ilmenite grains of the

886   micromineral assemblages of medium-grade fenite (Figure. 2b and Figure 2c) may be

887   caused by a simple oxidation of ilmenite that produces either these phases as stable end

888   products (Lindsley, 1963) or rutile together with a more Fe-rich ilmenite (Southwick, 1968).

889   Likewise, the magnetite grains with ilmenite lamellae found in low-grade fenite at Chilwa

890   Island (Figure 2a), may be formed by an 'oxyexsolution mechanism' (Wang et al., 2012;

891   Haggerty, 1991).

892

893   Lastly, in sample BM1968 P37 83, both monazite-(La) and monazite-(Ce) are present

894   (Figure 8a). Monazite may have formed in two phases. Analogously to monazite being more

895   common in reduced S-type granites than in oxidised I-granites, the more common monazite-

896   (Ce) may have crystallised first, with monazite-(La) forming later, when more oxidising

897   conditions led to Ce being in the 4^+ state, and therefore not able to be accommodated in

898   monazite. Alternative scenarios, such as Ce being taken up by allanite, or Ce^{4+} being taken

899   into cerianite, a mineral that may be formed as a late-stage weathering product, probably

900   did not operate at Chilwa Island, as neither of these minerals was identified. It is thought

901   more likely that Ce^{4+} did not participate in mineral formation, and was flushed out of the

902   system.

903

904   ***d.2 Fluids associated with silicification***

905   Fenitisation is generally associated with the elimination of free quartz (Pirajno, 2009), and

906   in general, quartz in the matrix of the fenites of this study decreases with degree of alteration.

907   However, secondary (recrystallised) quartz is present throughout medium-grade fenite and

908   breccia, with the high-grade sample BM1968 P37 83, wholly composed of this mineral,

909   representing an extreme example. Secondary quartz is also present in three of the four

910   carbonatites examined in this study, suggesting a role for autometasomatism and carbonate

911   replacement. Silicification is probably induced by the introduction of ground water (Garson

912   and Campbell Smith, 1958), with Si being dissolved and mobilised from country rock during

913   magma emplacement, and subsequently reprecipitated by fluids circulating in the complex.

914   It is therefore proposed that a Si-bearing fluid was the last metasomatising fluid event at

915   Chilwa Island, and occurred during waning carbonatite activity (Garson and Campbell Smith,

916   1958). Its action is often selective in nature and is commonly associated with REE

917   mineralisation at carbonatite complexes (Garson and Campbell Smith, 1958). The

918   relationship of silicification with carbonatite activity is supported by the high REE content of

919   the quartz high-grade fenite, the presence of quartz in carbonatite, and the association of

920   RE-minerals in veins of secondary quartz in medium/high-grade fenite samples. It is

921   recognised that silicification can be a weathering process, but this commonly results in the

922   formation of chalcedony rather than clean crystalline quartz. Furthermore, silicification by

923   weathering can have a diffuse effect, and create a cap to the carbonatite. The field relations

924   and mineralogical associations found at Chilwa Island would thus support hydrothermal

925   quartz.

926

927

928   **Fig. 12** Paragenetic sequence of fenite mineral formation associated with carbonatite emplacement and
929   metasomatism at Chilwa Island

930

EMPLACEMENT SEQUENCE

MINERALS	Sövite -related	Ankerite -related	Siderite -related	Post

Mineral precipitation

Possible mineral precipitation

Conclusions and implications

All three main carbonatites at the Chilwa Island complex are thought to have undergone magma boiling, leading to the expulsion of fluids that metasomatised the surrounding country rocks.

The nature of the fluid events produced by magma boiling is dependent on whether they derive from a first or second boiling. First magma boilings are associated with alkaline fluids and the pervasive formation of feldspar. Second boilings produce mineralising fluids that create microassemblages of minerals in veins.

During second boiling events, the REE were mobilised, transported and precipitated in the fluids that mineralised the fenites. REE fractionation took place, resulting in the formation of fenitic RE-bearing minerals with lower La/Nd ratios than their carbonatitic equivalents.

A suggested schematic model of the sequence of metasomatising fluids at Chilwa Island assigns elements mobilised in each event. Alkaline alteration of the whole aureole by fluids expelled from sövite was followed by mineralisation derived from ankerite carbonatite. A later alkaline event was more limited and strongly potassic, and occurred before further mineralisation associated with the 'sideritic' carbonatite. The aureole underwent later-stage silicification. The main features of this model regarding the nature of the multiple fluid events should be applicable to all alkaline-carbonatite complexes.

The presence of mineral assemblages in fenite at some distance from carbonatite could be developed as an exploration indicator of REE enrichment.

Bibliography

Andersen, T. (1989). Carbonatite-related contact metasomatism in the Fen complex, Norway: effects and petrogenetic implications. *Mineralogical Magazine , 53*, 395-414.

967 Andrade, F., Möller, P., Lüders, V., Dulski, P., & Gilg, H. (1999). Hydrothermal rare earth elements mineralisation
968 in the Barra do Itapirauã carbonatite, southern Brazil: behaviour of selected trace elements and stable isotopes
969 (C,O). *Chemical Geology , 155*, 91-113.

970 Bühn, B. (2008). The role of the volatile phase for REE and Y fractionation in low-silica carbonate magmas:
971 implications from natural carbonatites, Namibia. *Mineralogy and Petrology , 92*, 453-470.

972 Bühn, B., & Rankin, A. (1999). Composition of natural, volatile-rich Na-Ca-REE-Sr carbonatitic fluids trapped in
973 fluid inclusions. *Geochimica et Cosmochimica Acta , 63* (22), 3781-3797.

974 Bühn, B., Rankin, A., Radtke, M., Haller, M., & Knöchel, A. (1999). Burbankite, a (Sr,REE,Na,Ca)-carbonate in
975 fluid inclusions from carbonatite-derived fluids: Identification and characterisation using Laser Raman
976 spectroscopy, SEM-EDX and synchrotron micro-XRF analysis. *American Mineralogist , 84*, 1117-1125.

977 Bühn, B., Wall, F., & Le Bas, M. (2001). Rare-earth systematics of carbonatitic fluorapatites and their
978 significance for carbonatite magma evolution. *Contributions to Mineralogy and Petrology , 141*, 572-591.

979 Bailey, D. (1977). LIthospheric control of continental rift magmatism. *Geological Society of London Journal ,
980 133*, 103-106.

981 Belousova, E., Griffin, W., O'Reilly, S., & Fisher, N. (2002). Apatite as an indicator mineral for mineral
982 exploration: trace-element compositions and their relationship to host rock type. *Journal of Geochemical
983 Exploration , 76*, 45-69.

984 Brimhall, G., & Crerar, D. (1987). Ore fluids: magmatic to supergene. *Reviews in Mineralogy and Geochemistry
985 , 17*, 235-321.

986 Broom-Fendley, S., Wall, F., Brady, A., Gunn, A., Chenery, S., & Dawes, W. (2013). Carbonatite-hosted late-
987 stage apatite as a source of heavy rare earth elements? *12th SGA Biennial Meeting.*

988 Candela, P. (1997). A Review of Shallow, Ore-related Granites: Textures, Volatiles and Ore Metals. *Journal of
989 Petrography , 38* (12), 1619-1633.

990 Candela, P., & Blevin, P. (1995). Physical and chemical magmatic controls on the size of magmatic-
991 hydrothermal ore deposits. In A. Clark, *Giant Ore Deposits, II* (pp. 2-37). Kingston, Ontario, Canada: QMinEx
992 Associates and Queen's University.

993 Carmody, L. (2012). *Geochemical characteristics of carbonatite-related volcanism and subvolcanic
994 metasomatism at Oldoinyo Lengai, Tanzania.* London: University College of London, Earth Sciences.

995 Chakhmouradian, A., & Reguir, E. (2013). REE partitioning between crystals and melts: beyond the test tube.
996 *125th Anniversary of GSA.* Denver: GSA.

997 Chakhmouradian, A., & Wall, F. (2012). Rare earth elements: minerals, mines, magnets (and more). *Elements
998 , 8* (5), 333-340.

999 Cooper, A., & Paterson, L. (2008). Carbonatites from a lamprophyric dyke swarm, South Westland, New
1000 Zealand. *The Canadian Mineralogist , 46*, 753-777.

1001 Coulson, I., & Chambers, A. (1996). Patterns of zonation in Rare-earth-bearing minerals in nepheline syenites
1002 of the North Qôroq Centre, South Greenland. *The Canadian Mineralogist , 34*, 1163-1178.

1003 Dowman, E. (2014). *Mineralisation and fluid processes in the alteration zone around the Chilwa Island and
1004 Kangankunde carbonatite complexes, Malawi.* London: Kingston University.

1005 Drüppel, K., Hoefs, J., & Okrusch, M. (2005). Fenitising processes induced by ferrocarbonatite magmatism at
1006 Swartbooisdrif, NW Namibia. *Journal of Petrology , 46*, 377-406.

1007 Drake, M., & Weill, D. (1972). New rare earth element standards for electron microprobe analysis. *Chemical
1008 Geology , 10* (2), 179-181.

1009 Eby, G., Roden-Tice, M., Krueger, H., Ewing, W., Faxon, E., & Woolley, A. (1995). Geochronology and cooling
1010 history of the northern part of the Chilwa Alkaline Province, Malawi. *Journal of African Earth Sciences , 20* (3-
1011 4), 275-288.

Endurance Gold Corporation. (2012). *Bandito REE-Niobium Project, Yukon.* Retrieved 2013 йил 27-September from www.endurancegold.com: http://www.endurancegold.com/s/Bandito.asp

Endurance Gold Corporation. (2013, Jan). *The Bandito Intrusive Related Rare Earth-Niobium (Nickel-Copper)* ⌷OBJ⌷*Project,   Yukon.*   Retrieved   May   18,   2016   from   EnduranceGold.com: http://www.google.co.uk/url?sa=t&rct=j&q=&esrc=s&source=web&cd=5&ved=0ahUKEwjv6teX2eHMAhXEPRo KHQluC2kQFggxMAQ&url=http%3A%2F%2Fwww.endurancegold.com%2Fbandito%2Fedg_bandito_jan_201 3.pdf&usg=AFQjCNEPSHs8-5jt0cunh2jk4jpNVTdSLg&bvm=bv.122129774,d.d2s

Finch, A. (1995). Metasomatic overprinting by juvenile, igneous fluids, Igdlerfigsalik, South Greenland. *Contributions to Mineralogy and Petrology , 122*, 11-24.

Finch, A., & Walker, F. (1991). Cathodoluminescence and microporosity in alkali feldspar from the Blå Måne Sø perthosite, South Greenland. *Mineralogical Magazine , 55*, 583-589.

Garson, M. (1965). *Carbonatites in Southern Malawi.* Zomba, Malawi: The Government Printer.

Garson, M., & Campbell Smith, W. (1958). *Chilwa Island.* Zomba, Malawi: The Government Printer.

Gieré, R. (1996). Formation of rare earth minerals in hydrothermal systems. In W. F. Jones A, *Rare Earth Minerals* (pp. 105-150). London: Chapman & Hall.

Goodenough, K., Upton, B., & Ellam, R. (2000). Geochemical evolution of the Ivigtut granite, South Greenland: a fluorine-rich "A-type" intrusion. *Lithos , 51* (3), 205-221.

Haggerty, S. (1991). Oxide textures - a Mini-Atlas. *Reviews in Mineralogy and Geochemistry , 25*, 129-220.

Harlov, D. (2011). Formation of monazite and xenotime inclusions in fluorapatite megacrysts, Gloserheia Granite Pegmatite, Froland, Bamble Sector, southern Norway. *Mineralogy and Petrology , 102* (1-4), 77-86.

Harlov, D., & Förster, H.-J. (2003). Fluid-induced nucleation of (Y + REE)-phosphate minerals within apatite: Nature and experiment. Part II. Fluorapatite. *American Mineralogist , 88*, 1209-1229.

Hayward, C., & Jones, A. (1991). Cathodoluminescence petrography of Middle Proterozoic extrusive carbonatite from Qasiarsuk, South Greenland. *Mineralogical Magazine , 55*, 591-603.

Hetherington, C., Harlov, D., & Budzyń, B. (2010). Experimental metasomatism of monazite and xenotime mineral stability, REE mobility and fluid composition. *Mineralogy and Petrology , 99*, 165-184.

Hogarth, D. (1989). Pyrochlore, apatite and amphibole: distinctive minerals in carbonatite. In K. Bell, *Carbonatites: genesis and evolution* (pp. 105-148). London: Unwin Hyman.

Hoskin, P., Kinny, P., Wyborn, D., & Chappell, B. (2000). Identifying Accessory Mineral Saturation during Differentiation in Granitoid Magmas: an Integrated Approach. *Journal of Petrology , 41* (9), 1365-1396.

Hughes, J., & Rakovan, J. (2002). The crystal structure of apatite. *Reviews in Mineralogy and Geochemistry , 48*, 1-12.

Kempe, U., & Götze, J. (2002). Cathodoluminscence (CL) behaviour and crystal chemistry of apatite from rare-metal deposits. *Mineralogical Magazine , 66* (1), 151-172.

Keppler, H. (2003). Water solubility in carbonatite melts. *American Mineralogist , 88*, 1822-1824.

Keppler, H., & Wyllie, P. (1990). Role of fluids in transport and fractionation of uranium and thorium in magmatic processes. *Nature , 348*, 531-533.

Kröner, A., Willner, A., Hegner, E., Jaeckel, P., & Nemchin, A. (2001). Single zircon ages, PT evolution and Nd isotopic systematics of high-grade gneisses in southern Malawi and their bearing on the evolution of the Mozambique belt in southeastern Africa. *Precambian Research , 109*, 257-291.

Kresten, P., & Morogan, V. (1986). Fenitisation at the Fen complex, southern Norway. *Lithos , 19*, 27-42.

Le Bas, M. (1981). Carbonatite magmas. *Mineralogical Magazine , 44*, 133-140.

Le Bas, M. (1977). *Carbonatite-Nephelinite Volcanism.* New York: J Wiley & Sons.

Le Bas, M. (2008). Fenites associated with carbonatites. *The Canadian Mineralogist , 46*, 915-932.

Le Bas, M. (1987). Nephelinites and carbonatites. In U. B. Fitton J, *Alkaline igneous rocks* (pp. 53-84). Oxford: Blackwell.

1058   Le Bas, M. (1999). Sövite and alvikite: two chemically distinct calciocarbonatites C1 and C2. *South African*
1059   *Journal of Geology , 102*, 109-121.

1060   Leeman, W., & Phelps, D. (1981). Partitioning of rare earths and other trace elements between sanidine and
1061   co-existing volcanic glass. *Journal of Geophysical Research: Solid Earth , 86*, 10193-10199.

1062   Lindsley, D. (1963). Fe-Ti oxides in rocks as thermometers and oxygen barometers: Equilibrium relations of
1063   coexisting pairs of Fe-Ti oxides. *Carnegie I Wash , 1962-63*, 100-106.

1064   Lipin, B., & McKay, G. (1989). Geochemistry and Mineralogy of Rare Earth Elements. *Reviews in Mineralogy*
1065   *and Geochemistry , 21*, 1-348.

1066   Mariano, A. (1989). Nature of economic mineralisation in carbonatites and related rocks. In B. K, *Carbonatites:*
1067   *Genesis and Evolution* (pp. 147-176). Unwin Hyman.

1068   Mariano, A. (1988). Some further geological applications of cathodoluminescence. In D. Marshall,
1069   *Cathodoluminescence of geological materials* (pp. 112-113). Boston: Unwin Hyman.

1070   Mariano, A. (1978). The application of cathodoluminescence for carbonatite exploration and characterisation.
1071   In C. Brega (Ed.), *Proceedings of the First International Symposium on Carbonatites* (pp. 39-57). Brasil
1072   Departamento Nacional da Producao Mineral Brasilia.

1073   Mariano, A., & Ring, P. (1975). Europium-activated cathodoluminescence in minerals. *Geochimica et*
1074   *Cosmochimica Acta , 39* (5), 649-660.

1075   Mariano, A., Ito, J., & Ring, P. (1973). Cathodoluminescence of plagioclase feldspars. *Geological Society of*
1076   *America conference, Boulder, Colorado. 5*, p. 726. Boulder: Geological Society of America.

1077   Markl, G., Marks, M., & Frost, B. (2010). On the Controls of Oxygen Fugacity in the Generation and
1078   Crystallization of Peralkaline Melts. *Journal of Petrology , 51* (9), 1831-1847.

1079   Martin, R., Whitley, J., & Woolley, A. (1978). An Investigation of Rare-Earth Mobility: Fenitized Quartzites,
1080   Borralan Complex, N.W. Scotland. *Contributions to Mineralogy and Petrology , 66*, 69-73.

1081   McCreath, J., Finch, A., Simonsen, S., Donaldson, C., & Armour-Brown, A. (2012). Independent ages of
1082   magmatic and hydrothermal activity in alkaline igneous rocks: The Motzfeldt Centre, Gardar Province, South
1083   Greenland. *Contributions to Mineralogy and Petrology , 163* (6), 967-982.

1084   McKie, D. (1966). Fenitisation. In G. J. Tuttle O, *Carbonatites* (pp. 261-294). New York: Wiley Interscience.

1085   Migdisov, A., & Williams-Jones, A. (2014). Hydrothermal transport and deposition of the rare earth elements by
1086   fluorine-bearing aqueous liquids. *Mineralium Deposita , 49*, 987-007.

1087   Miles, A., Graham, C., Hawkesworth, C., Gillespie, M., & Hinton, R. (2013). Evidence for distinct stages of
1088   magma history recorded by the compositions of accessory apatite and zircon. *Contributions to Mineralogy and*
1089   *Petrology , 166*, 1-9.

1090   Mills, S., Kartashov, P., Kampf, A., Konev, A., Koneva, A., & Raudsepp, M. (2012). Cordylite-(La), a new mineral
1091   species in fenite from the Biraya Fe-REE deposit, Irkutsk, Russia. *The Canadian Mineralogist , 50* (5), 1281-
1092   1290.

1093   Morogan, V. (1989). Mass Transfer and REE mobility during fenitisation at Alnö, Sweden. *Contributions to*
1094   *Mineralogy and Petrology , 103*, 25-34.

1095   Morogan, V., & Woolley, A. (1988). Fenitisation at the Alnö carbonatite complex, Sweden: distribution,
1096   mineralogy and genesis. *Contributions to Mineralogy and Petrology , 100*, 169-182.

1097   Norton, G., & Pinkerton, H. (1997). Rheological properties of natrocarbonatites from Oldoinyo Lengai, Tanzania.
1098   *European Journal of Mineralogy , 9* (2), 351-364.

1099   Palmer, D. (1998). *The Evolution of Carbonatite Melts and their Aqueous Fluids: Evidence from Amba Dongar,*
1100   *India and Phalaborwa, South Africa.* Quebec: McGill University.

1101   Pirajno, F. (2009). *Hydrothermal Processes and Mineral Systems.* Perth, Australia: Springer.

1102   Platt, R., & Woolley, A. (1990). The carbonatites and fenites of Chipman Lake, Ontario. *The Canadian*
1103   *Mineralogist , 28*, 241-250.

1104 Portnov, A., & Gorobets, B. (1969). Luminescence of apatite from different rock types. *Dokl Akad Nauk USSR ,*
1105 *184*, 199-202.

1106 Rae, D., Coulson, I., & Chambers, A. (1996). Metasomatism in the North Qôroq centre, South Greenland: apatite
1107 chemistry and rare-earth element transport. *Mineralogical Magazine , 60*, 207-220.

1108 Robb, L. (2009). *Introduction to Ore-Forming Processes.* John Wiley & Sons.

1109 Rubie, D., & Gunter, W. (1983). The Role of Speciation in Alkaline Igneous Fluids duirng Fenite Metasomatism.
1110 *Contributions to Mineralogy and Petrology , 82*, 165-175.

1111 Rubin, J., Henry, C., & Price, J. (1993). The mobility of zirconium and other "immobile" elements during
1112 hydrothermal alteration. *Chemical Geology , 110*, 29-47.

1113 Shepherd, T., Rankin, A., & Alderton, D. (1985). *A practical guide to fluid inclusion studies.* Glasgow: Blackie &
1114 Son Ltd.

1115 Smith, M. (2007). Metasomatic silicate chemistry at the Bayan Obo Fe-REE-Nb deposit, Inner Mongolia, China:
1116 Contrasting chemistry and evolution of fenitising and mineralising fluids. *Lithos , 93*, 126-148.

1117 Smith, M., Henderson, P., & Campbell, L. (2000). Fractionation of the REE during hydrothermal processes:
1118 Constraints from the Bayan Obo Fe-REE-Nb deposit, Inner Mongolia, China. *Geochimica et Cosmochimica*
1119 *Acta , 64* (18), 3141-3160.

1120 Smith, M., Henderson, P., & Peishan, Z. (1999). Reaction relationships in the Bayan Obo Fe-REE-Nb deposit
1121 Inner Mongolia, China: implications for the relative stability of rare-earth element phosphates and
1122 fluorocarbonates. *Contributions to Mineralogy and Petrology , 134*, 294-310.

1123 Snelling, N. (1965). Age determinations on three African carbonatites. *Nature , 205*, 491.

1124 Southwick, D. (1968). Mineralogy of a rutile- and apatite-bearing ultramafic chlorite rock, Harford County,
1125 Maryland. *Geological Survey Research , 600-C*, C38-C44.

1126 Sverjensky, D. (1984). Europium redox equilibria in aqueous solution. *Earth and Planetary Science Letters , 67*
1127 (1), 70-78.

1128 Vartiainen, H., & Woolley, A. (1976). The petrography, mineralogy and chemistry of the fenites of the Sokli
1129 intrusion, Finland. *Geological Survey of Finland Bulletin , 280*, 1-87.

1130 Verplanck, P., & Van Gosen, B. (2011). *Carbonatite and Alkaline Intrusion-Related Rare Earth Element Deposits*
1131 *- A Deposit Model.* Retrieved 08 01, 2013 from USGS: http://pubs.usgs.gov/of/2011/1256/report/OF11-1256.pdf

1132 Verschure, R., & Maijer, C. (2005). A new Rb-Sr isotopic parameter for metasomatism, $\triangle$t, and its application in
1133 a study of pluri-fenitised gneisses around the Fen ring complex, South Norway. *Norges geologiske*
1134 *undersøkelse, Bulletin , 445*, 45-71.

1135 Viladkar, S. (2012). Evolution of Calciocarbonatite Magma: Evidence from the Sövite and Alvikite Association
1136 in the Amba Dongar Complex, India. In D. Panagiotaras (Ed.), *Geochemistry -Earth's System Processes* (pp.
1137 485-500). In Tech.

1138 Voron'ko, Y., Gorbachev, A., Zverev, A., Sobol, A., Morozov, N., & Murav'ev, E. e. (1992). Raman scattering
1139 and luminescence spectra of compounds with the structure of apatite $Ca_5(PO_4)_3F$ and $Ca_5(PO_4)_3OH$ activated
1140 with Eu^{3+} ions. *Neorganicheskie Materialy , 28*, 582-589.

1141 Wall, F. (2000). *Mineral chemistry and petrogenesis of rare earth-rich carbonatites with particular reference to*
1142 *the Kangankunde carbonatite, Malawi.*

1143 Wang, R., Yu, A.-P. C., Xie, L., Lu, J.-J., & Zhu, J.-C. (2012). Cassiterite exsolution with ilmenite lamellae in
1144 magnetite from the Huashan metaluminous tin granite in southern China. *Mineralogy and Petrology , 105*, 71-
1145 84.

1146 Waychunas, G. (2002). Luminescence of Natural and Synthetic Apatites. *Reviews in Mineralogy and*
1147 *Geochemistry , 48* (1), 701-742.

1148   Williams-Jones, A., & Palmer, D. (2002). The evolution of aqueous-carbonic fluids in the Amba Dongar
1149   carbonatite, India: implications for fenitisation. *Chemical Geology , 185*, 283-301.
1150   Woolley, A. (1982). A discussion of carbonatite evolution and nomenclature, and the generation of sodic and
1151   potassic fenites. *Mineralogical Magazine , 46*, 13-17.
1152   Woolley, A. (2001). *Alkaline Rocks and Carbonatites of the World Part 3: Africa.* London: The Geological
1153   Society.
1154   Woolley, A. (1969). Some aspects of fenitisation with particular reference to Chilwa Island and Kangankunde,
1155   Malawi. *Bulletin British Museum of Natural History (Mineralogy) , 2* ((4)), 191-219.
1156   Woolley, A., & Kempe, D. (1989). Carbonatites: nomenclature, average chemical composition and element
1157   distribution. In K. Bell, *Carbonatites: Genesis and Evolution* (pp. 1-14). London: Unwin Hyman.
1158   Zaitsev, A., Wall, F., & Le Bas, M. (1998). REE-Sr-Ba minerals from the Khibina carbonatites, Kola Peninsula,
1159   Russia: their mineralogy, paragenesis and evolution. *Mineralogical Magazine , 62* (2), 225-250.
1160